DOE/NASA/0067-79-2
NASA CR-159705

TECHNOLOGY DEVELOPMENT FOR PHOSPHORIC ACID FUEL CELL POWERPLANT (PHASE II): 3RD QUARTERLY REPORT

LARRY CHRISTNER
ENERGY RESEARCH CORPORATION

JUNE 1979

PREPARED FOR
NATIONAL AERONAUTICS AND SPACE ADMINISTRATION
LEWIS RESEARCH CENTER
UNDER CONTRACT DEN3-67

FOR
U.S. DEPARTMENT OF ENERGY
ENERGY TECHNOLOGY
DIVISION OF FOSSIL FUEL UTILIZATION

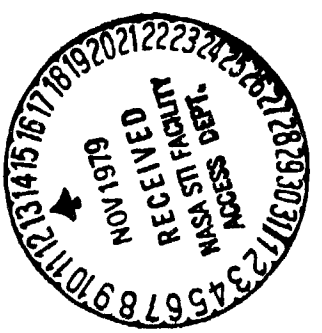

DOE/NASA/0067-79/2
NASA CR-159705

TECHNOLOGY DEVELOPMENT FOR PHOSPHORIC ACID FUEL CELL POWERPLANT (PHASE II): 3RD QUARTERLY REPORT

LARRY CHRISTNER
ENERGY RESEARCH CORPORATION
3 GREAT PASTURE ROAD
DANBURY, CONNECTICUT 06810

JUNE 1979

PREPARED FOR
NATIONAL AERONAUTICS AND SPACE ADMINISTRATION
LEWIS RESEARCH CENTER
CLEVELAND, OHIO 44135
UNDER CONTRACT DEN3-67

FOR
U.S. DEPARTMENT OF ENERGY
ENERGY TECHNOLOGY
DIVISION OF FOSSIL FUEL UTILIZATION
WASHINGTON, D.C. 20545
UNDER INTERAGENCY AGREEMENT DE-AI-03-79 ET11272

EXECUTIVE SUMMARY

Component Development

- A technique for producing an acid inventory control member (AICM) by spraying FEP onto a partially screened carbon paper backing has been developed. Further development of this promising technique will continue.
- The acid pick-up of all components has been measured and the volume changes of electrolyte during stack operation have been estimated to aid in determining the acid storage capacity needed in the AICM.
- Carbonization of bipolar plate materials has been successfully achieved without blistering.
- Preliminary evaluation of 30.5 cm x 43.2 cm sheet mold electrodes tested in 350 cm^2 stacks indicates acceptable performance level: Stack 379 showed an initial performance of 0.64V/cell at 100 ASF.

Materials Evaluation

- Corrosion resistance tests for a series of thermoplastics at 185°C have shown that polyphenylsulfone is the least vulnerable to acid.
- SEM examination of resin materials after exposure to acid shows surface etching.
- A detailed evaluation of various factors contributing to the ohmic resistance of a cell suggests that contact resistance is a major factor.

Endurance Testing

- Ohmic resistance has been reduced to improve performance by systematic compression of the stacks.

ENERGY RESEARCH CORPORATION

TABLE OF CONTENTS

Section		Page No.
	EXECUTIVE SUMMARY	i
TASK I.	COMPONENT DEVELOPMENT	1
1.1	Matrix Development	1
1.2	Electrode Scale-Up	5
1.3	Definition and Control of Electrolyte Volume Changes	5
1.4	Bipolar Plate Technology	20
TASK II.	MATERIAL EVALUATION	23
2.1	Component Corrosion Resistance	23
2.2	Physical Property Measurements	27
2.3	Estimation of Cell Component Resistance	27
TASK III.	ENDURANCE TESTING	34
3.1	Prediction of P_4O_{10} Vapor Concentration	34
3.2	Measurement of P_4O_{10} Vapor Concentration	36
3.3	Effect of Operating Variables on Cell Performance	39
3.3.1	Effect of Compression on the Stack	39
3.3.2	Effect of Reformed Fuel	47
3.3.3	Effect of Current Density	49
3.3.4	Preheated Hydrogen	49
3.4	Component Evaluation	50
3.4.1	Effect of Teflon in Electrodes	50
3.4.2	Sheet Mold Electrodes	53
3.4.3	Wet Assembly of SiC Matrix Stacks	53
TASK IV.	SHORT STACK TESTING	56
	APPENDIX A Estimation of Cell Component Resistances	59

LIST OF FIGURES

Section			Page No.
TASK I.		COMPONENT DEVELOPMENT	
	I.1	SEMs of SiC Matrices	4
	I.2	Electrolyte Concentration Changes with Temperature at Various Humidity Conditions	7
	I.3	Volume Change with Ambient Moisture Conditions During Electrode Cooling	8
	I.4	Acid Pick-up in Electrode with Elapsing Time	11
	I.5	Comparison of Acid Pick-up in Compressed Rolled Electrodes with Elapsing Time	13
	I.6	Electrode Acid Pick-up from Wet Matrix with Elapsed Time	15
	I.7	AICM Acid Pick-up in Backing Papers with Elapsed Time	19
	I.8	Shrinkage in Carbonized Graphite/Colloid 8440 Resin	21
	I.9	Shrinkage in Carbonized Graphite/Varcum 24-655 Resin	22
TASK II.		MATERIAL EVALUATION	
	II.1	Weight Changes During and After H_3PO_4 Exposure	24
	II.2	Observable Weight Changes in Graphite/Resin	25
	II.3	Acid Corrosion of 68% Graphite/32% Colloid 8440 (Sample #389A in 180°C H_3PO_4)	26
	II.4	SEMs of 100% Colloid 8440 Resin with no Acid Exposure (Sample 357-03)	28
	II.5	SEMs of 100% Colloid 8440 Resin After 1500 Hours of 185°C H_3PO_4 Exposure (Sample 357-A)	28
	II.6	SEMs of 100% Varcum 24-655 Resin After 2250 Hours of 185°C H_3PO_4 Exposure (Sample 349-1B)	29

LIST OF FIGURES (Concluded)

Section		Page No.
TASK III.	ENDURANCE TESTING	
III.1	P_4O_{10} Vapor Concentration Predicted by Tlnν = Constant	37
III.2	Ohmic Resistance as a Function of Temperature	48
III.3	Ohmic Resistance as a Function of Compression	48
III.4	Temperature Distribxtion for Room Temperature and Preheated H_2 (Stack 381, Cell #2)	51
III.5	Lifegraphs of Stacks 366 and 367	52
III.6	Lifegraph for Stack 379	54
TASK IV.	SHORT STACK TESTING	
IV.1	Lifegraph for Stack 406	58
	APPENDIX A Estimation of Cell Component Resistances	
A-1	Exploded View of Component Resistances in a Fuel Cell Stack	60
A-2	Schematic View of a Bipolar Plate Element	62

LIST OF TABLES

Section		Page No.
TASK I.	COMPONENT DEVELOPMENT	
I.1	Cell Testing Summary	2
I.2	Steps to Estimate Volume Change	6
I.3	Electrolyte Volume Changes During Stack Preparation (12.7 cm x 38.1 cm Cells)	9
I.4	Acid Pick-up of Electrodes Wicked From Matrices (All Data Corrected for Concentration of Acid)	16
I.5	Comparison of Perforated Screens for AICM Production	17
TASK II.	MATERIAL EVALUATION	
II.1	Component Corrosion Resistance to 185°C H_3PO_4	30
II.2	Increase in Resistivity of Graphite/Resin with Addition of Asbury 850 Graphite	31
II.3	Estimated Resistance of Cell Components (12.7 cm x 38.1 cm [5 in. x 15 in.] Stack)	32
TASK III.	ENDURANCE TESTING	
III.1	P_4O_{10} Concentration Predicted Using Equilibrium Data (302 to 370°C Range)	35
III.2	P_4O_{10} Concentrations Extrapolated from Normal Boiling Point Data	38
III.3	Measured P_4O_{10} Vapor Concentrations	40
III.4	Stack Testing Summary	41
III.5	Performance of Wet-Assembled SiC Stacks	55
TASK IV.	SHORT STACK TESTING	
IV.1	Summary of Stacks 406 and 407	57

TASK I. COMPONENT DEVELOPMENT

1.1 Matrix Development

Efforts to improve the strength and handleability of the SiC matrix have continued. One technique which has been discussed previously is that of sintering the matrix and electrode at the same time. A matrix was cast onto an unsintered electrode and preheated at 225°C for 40 minutes, then sintered at 350°C for 25 minutes. The result is a strong matrix that is tightly bonded to the electrode. The question of whether matrix or electrode performance would be adversely affected by such a sintering technique was investigated with Cell #1294. The cell ran well for over 2000 hours before termination (See Table I.1). The combined sintering technique would, therefore, appear to be a viable technique for enhancing the physical strength of the matrix as well as for reducing the handling and oven time required for electrode and matrix operations.

Another technique for strengthening the matrix which has been mentioned previously is to increase the amount of plastic in the inking vehicle. In order to increase the amount of plastic in the matrix without producing a slurry too viscous to mix or cast, a lower molecular weight grade of the same material presently in use was tried. The concentration of this plastic in the inking vehicle was 2.5% versus 0.5% for the higher molecular weight grade. The result was a matrix strong enough to be cut to shape with a steel rule die without crumbling or flaking off. The matrix is safe and easy to handle up to the sintering process, during which time most, if not all, of the plastic burns off. After sintering, the matrix appears to be at least as strong as a matrix made with the standard inking vehicle, the porosity is greater (64 to 68%) and the bubble pressure is good (125 to 140 kPa). Cell #1328 contains a cathode coated with a SiC matrix made with a 2.5% plastic inking vehicle. The performance peaked at 740 mV (IR free) at 100 mA/cm^2 and is presently running 690 mV (IR free) at 200 mA/cm^2 after more than 600 hours. Cell #1295 contained a similar

TABLE I.1

CELL TESTING SUMMARY

CELL NO.	1278	1294	1295	1307	1316	1328	1341
TEST OBJECTIVE	Anode Backing Test	Matrix & Electrode Sintered Together	Matrix (Higher Plastic Content)	Compressed Electrodes, 690 kPa	Anode Backing Test	Matrix (Higher Plastic Content)	AICM
CELL CHARACTERISTICS							
ANODE							
TYPE	Rolled	Rolled	Rolled	Rolled	Rolled	Rolled	Rolled
TFE, %	40	40	40	40	40	40	40
LOADING, mg Pt/cm^2	0.32	0.3	0.3	0.3	0.3	0.31	0.3
CATHODE							
TYPE	Rolled	Rolled	Rolled	Rolled	Rolled	Rolled	Rolled
TFE, %	40	40	40	40	40	40	40
LOADING, mg Pt/cm^2	0.5	0.5	0.3	0.5	0.5	0.78	0.5
MATRIX	SiC	SiC	SiC	Kynol	SiC	SiC	SiC
TFE, %	4	4	4	-	4	4	4
POROSITY, %	33	-	64	-	-	-	-
THICKNESS, cm	0.015	0.018	0.018	0.046	0.015	0.013	0.015
SINTERING	25 min @ 275°C	40 min @ 225°C 25 min @ 350°C	15 min @ 330°C	-	15 min @ 330°C	15 min @ 330°C	40 min @ 225°C 25 min @ 350°C
ANODE BACKING, % FEP	20	39	39	35	28	39	9
CATHODE BACKING, % FEP	40	36	37	35	37	35	36
PERFORMANCE (IR FREE)							
AIR @ 100 mA/cm^2							
PEAK, mV	723	715	680	675	715	740	530
AVERAGE, mV	670	675	660	665	695	730	-
PRESENT, mV	•	•	•	•	670	720	•
AIR @ 200 mA/cm^2							
PEAK, mV	670	655	560	615	665	710	-
O_2 @ 100 mA/cm^2 (Peak)	780	765	740	750	775	810	-
CELL LIFE, hrs.	3528	2012	1368	336	1080	744	24

• Test terminated.

matrix made with a 3% plastic inking vehicle. If additional testing verifies that the increased plastic in the matrix does not harm cell performance, then this matrix will become our new standard.

To learn more about what happens to a matrix at the microscopic level during sintering, samples of both sintered and unsintered matrices were examined with a scanning electron microscope (SEM). Figure I.1a shows an unsintered SiC matrix magnified 10,000X. The large, irregular particles are SiC and the smaller, spheroidal particles are PTFE. The PTFE can be seen clinging to the sides of the SiC and partially filling the gaps between particles. Since there is only 4 wt% PTFE in this particular sample, a cluster this large probably represents a poor distribution. It took over an hour of searching on this sample to find a group of particles this distinct, and most of the PTFE appeared to be more evenly dispersed. Figures I.1b, I.1c and I.1d are pictures of a similar matrix which has been sintered at 350°C for 15 minutes. It was hoped that by comparing the extreme case of a sintered matrix with an unsintered one, some general conclusions could be drawn about the effects of sintering on the matrix. Figure I.1b shows how the PTFE particles have flowed together to form elongated "puddles". In Figure I.1c, taken elsewhere in the same sample, PTFE can be seen clinging to the sides of the SiC and bridging the gap between particles. Figure I.1d is an enlargement of the center portion of Figure I.1c. In the last three figures, it appears that, although the sintered PTFE did flow at the sintering temperature, the flow did not produce large, nonwettable films of PTFE on the SiC particles.

As explained in previous reports, the sintering conditions must balance considerations for wicking ability (which is greater at lower sintering temperatures) with the need for strength and high bubble pressure. Originally matrices were sintered to maximize their wicking ability, but over a period of time it became apparent from testing several 12.7 cm x 38.1 cm stacks (e.g. Nos. 380, 381, 385 and 387) that wicking was still adequate at higher

a. Unsintered 10,000X

P0121a

b. Sintered at 350°C 20,000X

P0121b

c. Sintered at 350°C 10,000X

P0121c

d. Sintered at 350°C 30,000X

P0121d

FIGURE I.1 SEMS OF SiC MATRICES

sintering temperatures.

1.2 Electrode Scale-Up

Production of 45.7 cm x 45.7 cm (18 in. x 18 in.) sheet molded electrodes is continuing. There have been some problems in obtaining an even distribution of catalyst material over the large area, but most of these problems appear to have been solved. Most electrodes are now being held to within ±0.006 cm (±0.0025 in.) thickness across their surface, which is approximately the same dimensional tolerance accepted in the underlying carbon paper backings. The variations are usually localized high spots which can be shaved with a razor blade to acceptable dimensions. Procedures are being developed to eliminate this occasional problem. The electrodes have been tested in two 12.7 cm x 38.1 cm (5 in. x 15 in.) stacks. The performance of Stacks 379 and 384 is described in Section III.4, Component Evaluation.

1.3 Definition and Control of Electrolyte Volume Changes

- Volume Changes During Stack Assembly
  Electrolyte volume changes in a fuel cell under various temperature and humidity conditions have been estimated as shown in Table I.2.

Figure I.2 shows variation of electrolyte concentration with temperature in equilibrium at various humidity conditions. The curves were prepared from literature data* and are used to estimate electrolyte volume changes. Figure I.3 shows volume change curves for T = 77°C and four other temperatures as a function of partial pressure of moisture in the environment. Table I.3 illustrates a numerical example of volume changes during 12.7 cm x 38.1 cm (5 in. x 15 in.) cell preparation for a typical set of conditions. As shown, a large amount of acid will be squeezed out

* Striplin, Ind. & Eng. Chem. 33, 912 (1941).
Fontana, J., Am. Chem. Soc., 73, 3348 (1951).
Christensen & Reed, Ind. & Eng. Chem. 47, 1277 (1955).
McDonald & Boyack, J. Chem. Eng. Data 14 (3), 380 (1969).

TABLE I.2. STEPS TO ESTIMATE VOLUME CHANGE

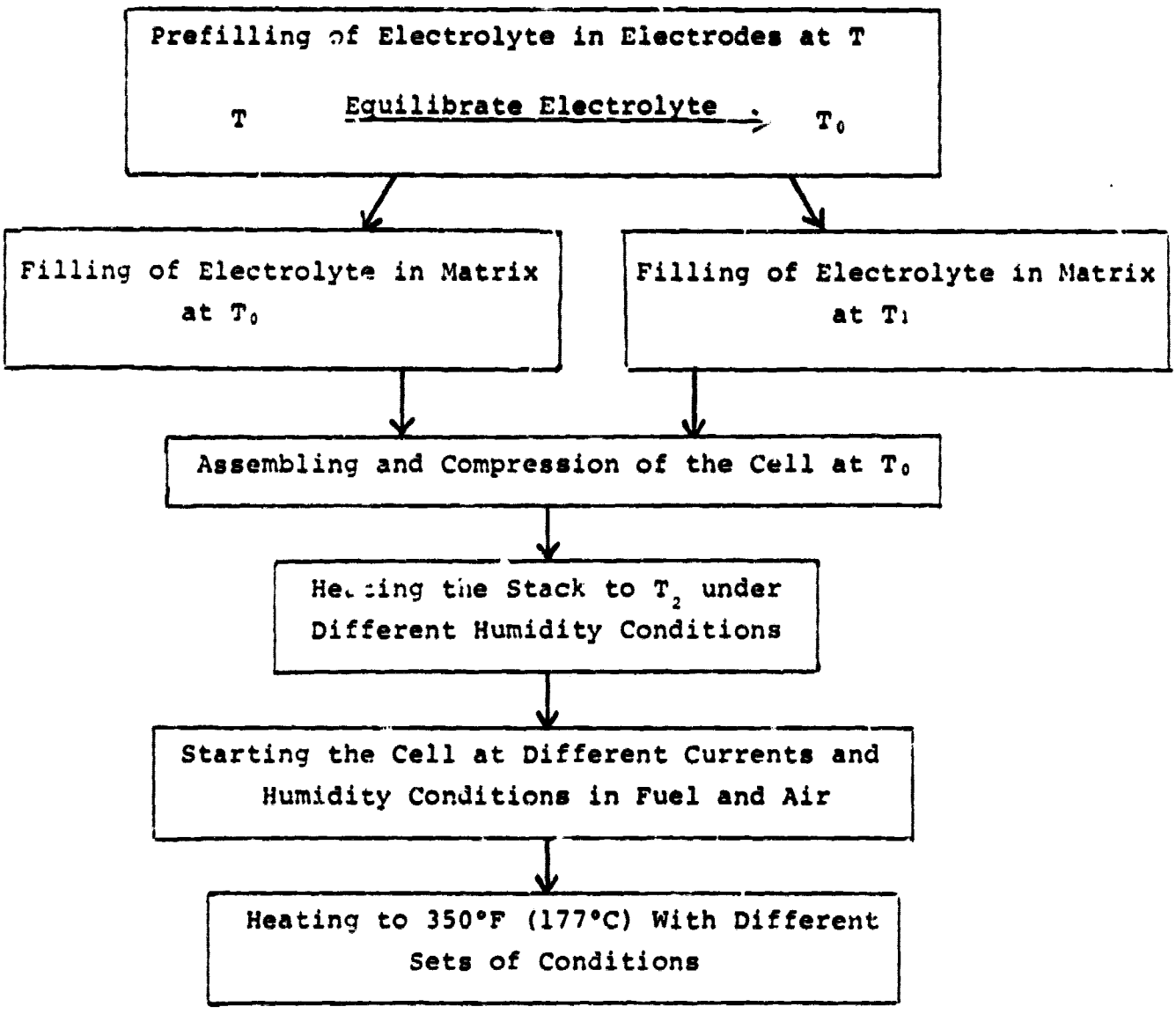

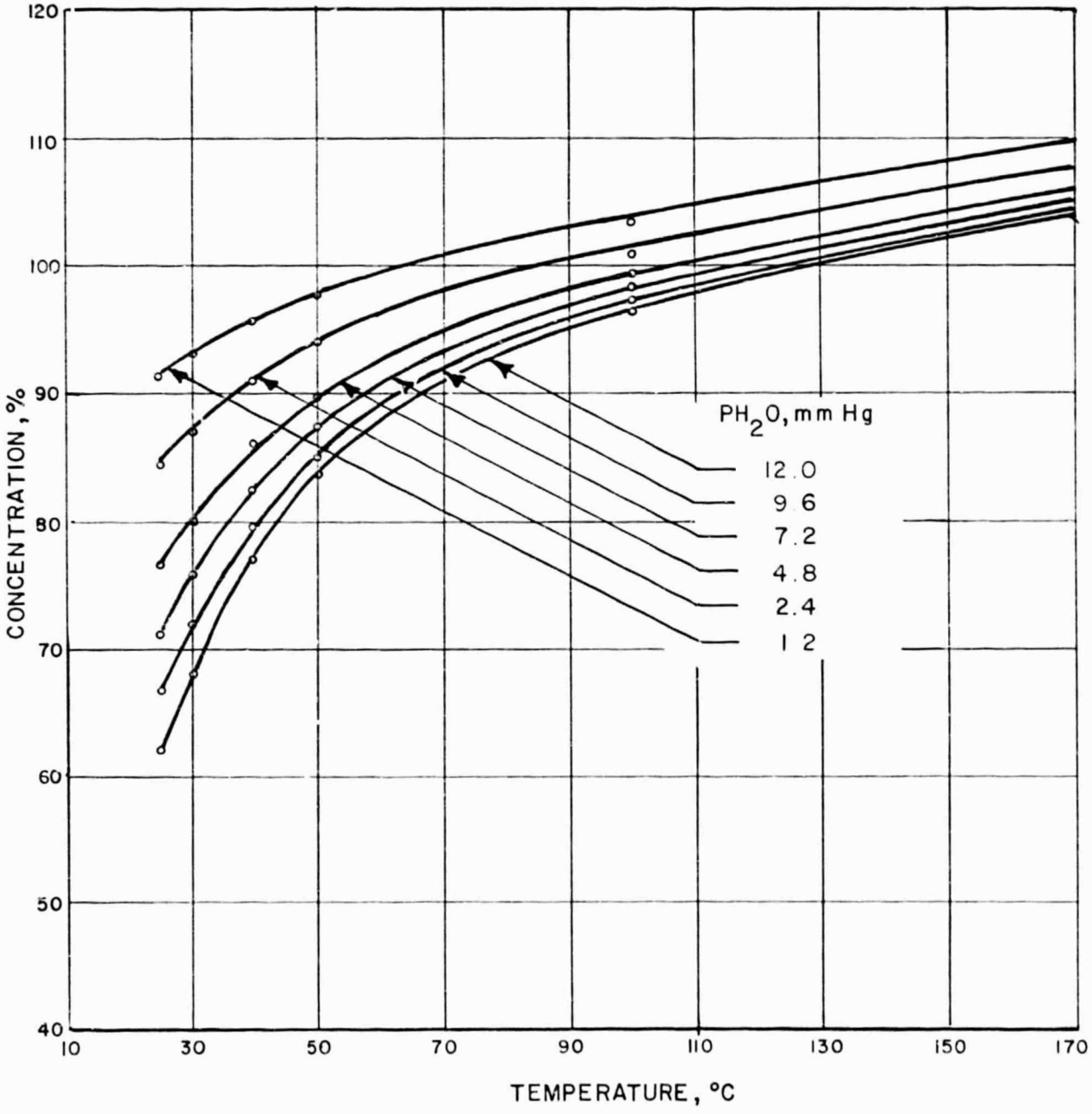

FIGURE I.2. ELECTROLYTE CONCENTRATION CHANGES WITH TEMPERATURE AT VARIOUS HUMIDITY CONDITIONS

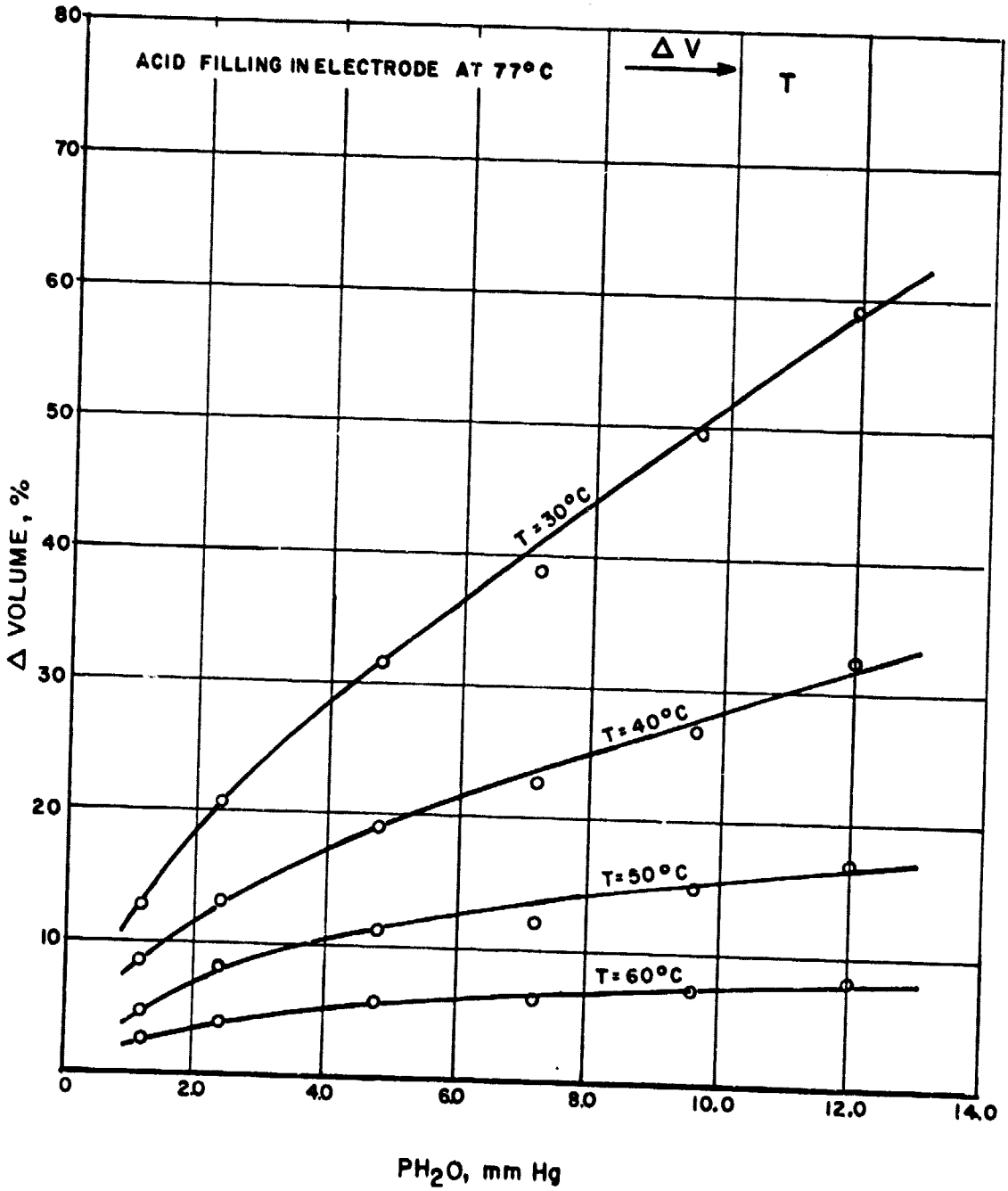

FIGURE I.3. VOLUME CHANGE WITH AMBIENT MOISTURE CONDITIONS DURING ELECTRODE COOLING

ENERGY RESEARCH CORPORATION

TABLE I.3 ELECTROLYTE VOLUME CHANGES DURING STACK PREPARATION*
(12.7 cm x 38.1 cm cells)

(Based on P_{H_2O} = 1.2 mm Hg in Dry Room)

(A) Filling of Electrolyte in Electrodes at 77°C in Oven

Acid Concentration = 101.5%, Volume of Acid = 2.12 cm^3 in Electrode

ΔV_{AB} = 13% in Electrode | ΔV_{AB} = 0.28 cm^3 in Electrode

(B) (1) Cooling of Electrodes to 30°C (P_{H_2O} = 1.2 mm Hg)

Acid Concentration = 93%, Volume of Acid = 2.4 cm^3 in Electrode

(2) Filling of Acid in Matrix at 30°C

Acid Concentration = 100%, Saturated Volume of Acid = 15.63 cm^3 in Matrix

Thickness of Electrode = 0.018 cm / Thickness of Matrix = 0.0544 cm

Total Acid 18.03 cc

ΔV_{BC} = 20.7% | ΔV_{BC} = -3.73 cm^3 (squeezed out)

(C) Compression of Cell at 90 psia at 30°C, P_{H_2O} (in dry room) = 1.2 mm Hg

Thickness of Electrode = 0.014 cm / Thickness of Matrix = 0.0434 cm

Acid Concentration = 98.29% (Volume Averaged), Volume of Acid = 14.3 cm^3

ΔV_{CD} = -7.9% | ΔV_{CD} = -1.13 cm^3

(D) Heating to 121°C (250°F), Under P_{H_2O} = 1.2 mm Hg

Acid Concentration = 105.8%, Acid Volume = 13.17 cm^3

ΔV_{DE} = 17.67% | ΔV_{DE} = 2.95 cm^3

(E) Starting the Cell and Heating to 177°C (350°F)

DIGAS Process: P_{H_2O} = 195 mm Hg in Cathode Channels,

P_{H_2O} = 97.5 mm Hg in Anode Channels at I = 150 ASF

Acid Concentration = 97.8%, Acid Volume = 16.12 cm^3

* ΔV_{ij} = Volume Change Between Steps i and j.

under pressure if the matrices are saturated with acid before compression. Therefore the amount of acid to be put in a matrix should be the saturated minus ΔV_{BC} (i.e., 15.63 - 3.73 = 11.9 cm^3) for the example case. Once the cell is assembled and compressed, the stack will undergo a total volume change of 1.82 cm^3 until it reaches a steady operating condition. This amount of volume will be the size of the AICM to be built inside the stack.

- Acid Pick-Up in Electrodes

A number of different kinds of acid pick-up tests have been conducted. These include float filling, vacuum (float) filling, and wicking from a matrix. These tests have been performed under a variety of conditions. Some samples are checked periodically in order to establish rates of acid pick-up and other samples are weighed only at the end of the tests to measure the final pick-up. For these reasons, some of the data is presented graphically and some is presented in tabular form. All of the data has been corrected to allow for the concentration changes in the acid occurring during the test.

In the first series of float filled electrodes, small samples (5.1 cm x 5.1 cm) were cut from the same 12.7 cm x 38.1 cm rolled electrode. They were tested in duplicate under the conditions listed in Figure I.4.

Since the acid adsorption results from two duplicate samples did not deviate from the average by more than 0.25 x 10^{-3} cm^3/cm^2, only the averages are shown in Figure I.4.

Data for Sample AB has been presented before and is included here for comparison only. Because only two data points (plus the origin) were taken for Sample AB, dotted lines were drawn rather than trying to assume the shape of a curve. In this test, as in all of the float filling tests, the electrode samples were placed with catalyst side down in a beaker of acid and then placed in an oven at the temperature listed on the figure. Sometimes the acid

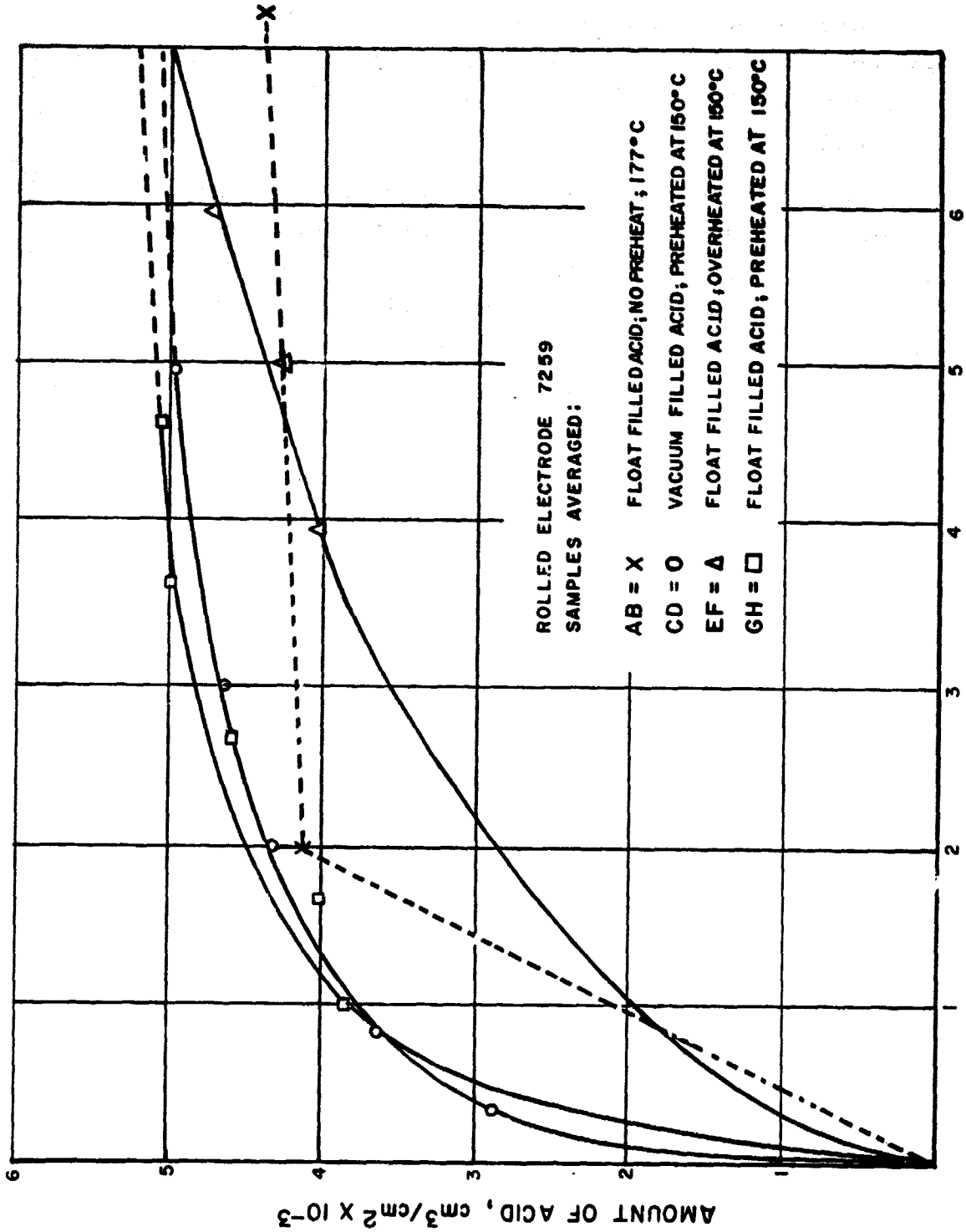

FIGURE I.4. ACID PICK-UP IN ELECTRODE WITH ELAPSING TIME

D0693

was preheated for one hour prior to the test as listed in Figure I.4). Whenever it was time to weigh a sample, the electrodes were removed from the oven one at a time, gently blotted on Aldex paper to remove excess surface acid and then quickly weighed on a digital scale.

Sample CD illustrates acid pick-up of electrodes float filled in a vacuum oven. It had been hoped that applying a vacuum would greatly speed up the electrode filling process, but these results indicate that vacuum filling of electrodes is probably not worth the effort: it seems to speed up the early stages of electrode filling but, after the first hour or so, the rate of fill tapers off to that of other float filled electrodes. The comparison is quite apparent in Figure I.4. Dissection of 12.7 cm x 38.1 cm stacks has revealed that some of the electrode backings are being compressed to such an extent that they are crushed by the ribs of the bipolar plates. The rib pattern can be clearly seen impressed upon the backings and these indented areas are prone to electrolyte flooding. In an effort to determine how much of a problem this flooding might be, two electrodes (a 0.3 mg Pt/cm^2 anode and a 0.5 mg Pt/cm^2 cathode) were deliberately compressed between two bipolar plates. The electrodes were cut in half and then arranged between the bipolar plates as they would be in a cell. The units were then placed in a small press and one set of half electrodes was compressed at 70 psi (483 kPa) while the other set was compressed at 100 psi (690 kPa). Small samples cut from the electrode halves were then float filled as in previous tests. Figure I.5 shows the rate of acid pick-up of the samples compared with the graph of the average of Samples A and B from the previous tests. A and B were of a loading similar to that of the cathode used in this test. The data indicates that the cathodes absorbed more acid than the anodes, which is to be expected because the higher loaded cathode has a thicker catalyst layer. The cathodes, compressed at 483 kPa and 690 kPa, picked up

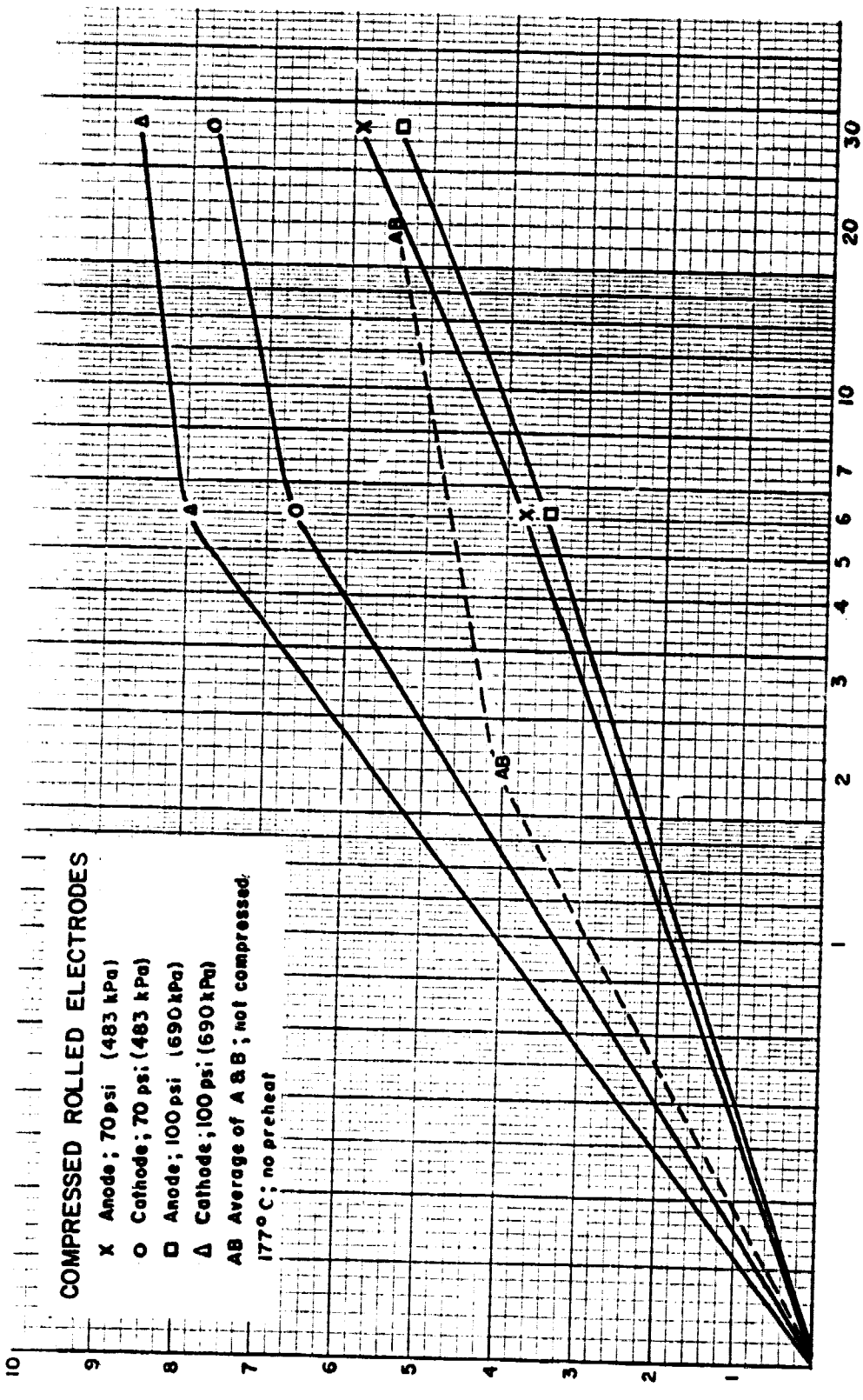

FIGURE I.5 COMPARISON OF ACID PICK-UP IN COMPRESSED ROLLED ELECTRODES WITH ELAPSING TIME

D0694

40% and 60% more acid, respectively, than did the uncompressed sample in the same time period. The graph for the uncompressed AB falls between that of the cathodes and the anodes. The cathode compressed at 690 kPa absorbed more acid than the cathode compressed at 483 kPa, which was also expected. However the anode compressed at 690 kPa picked up slightly less acid than the anode compressed at 483 kPa. The reason for this reversal of the expected order is not known. Similar tests are planned. Cell #1307 was built with electrodes compressed at 690 kPa (Table I.1). Cell performance was mediocre and began to deteriorate fairly soon. After two weeks, the cell was disassembled. The cathode backing showed moderate flooding in the compressed rib area but the anode backing gave no signs of being flooded.

The other kind of acid pick-up test involved wicking electrodes from acid-soaked matrices, as would normally be done in cell construction. Some tests were done on small (5.1 cm x 5.1 cm) samples and other tests were performed on full size 12.7 cm x 38.1 cm (5 in. x 15 in.) and 30.5 cm x 43.2 cm (12 in. x 17 in.) electrodes. In this type of test, an acid-soaked Kynol matrix was placed between two electrodes, forming a sandwich. Weights were placed on top of the sandwich and the whole unit was placed in the oven. Figure I.6 shows one such test where samples were all cut from the same electrode. The graph shows that in both cases the electrode on the bottom of the sandwich picked up more acid than the electrode on top. This trend holds in most of the tests of this type. Table I.4 lists the conditions and results of other tests performed. Electrode filling is slower when wicking from a matrix than when float filling, but the ultimate pick-up appears to be similar.

These tests indicate that in a stack, a 12.7 cm x 38.1 cm (5 in. x 15 in.) uncompressed electrode with typical 0.5 mg Pt/cm^2 could be expected to hold approximately 2.0 cm^3 of acid and a similarly loaded 30.5 cm x 43.2 cm (12 in. x 17 in.) electrode would hold approximately 5.3 cm^3.

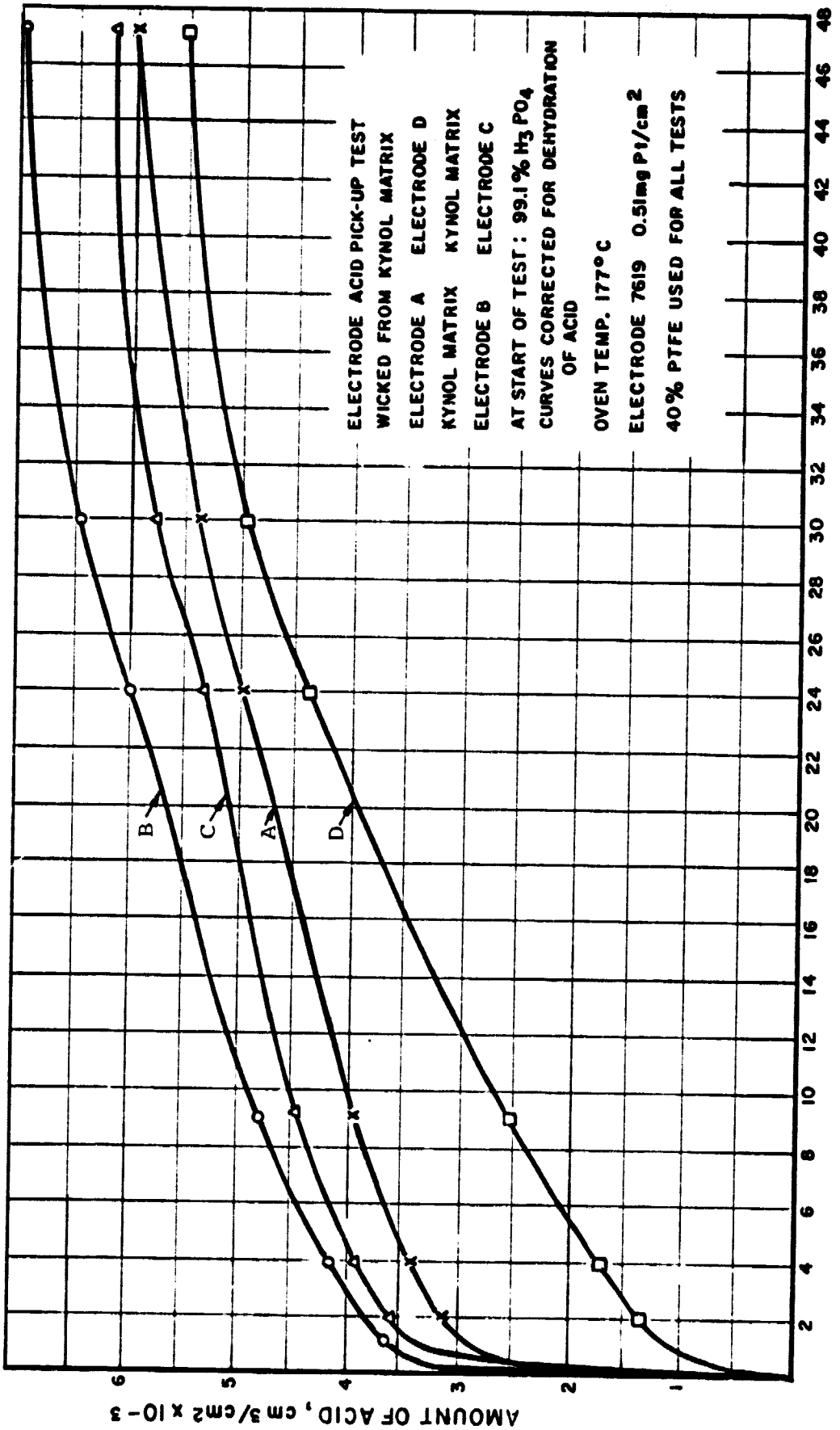

FIGURE I.6 ELECTRODE ACID PICK-UP FROM WET MATRIX WITH ELAPSED TIME

D0695

TABLE I.4

ACID PICK-UP OF ELECTRODES WICKED FROM MATRICES

(All Data Corrected for Concentration of Acid)

SAMPLE	SIZE, cm	MATRIX	TIME, days	TEMP, °C	PICK-UP, $cm^3/cm^2 \times 10^{-3}$
0.67 mg Pt/cm^2 rolled electrodes 40% PTFE					
1A Top	12.7 x 38.1	Kynol	7	150	4.42
1B Bottom	12.7 x 38.1	Kynol	7	150	4.24
0.9 mg Pt/cm^2 rolled electrodes 40% PTFE					
5960 Top	12.7 x 38.1	Kynol	5	150	6.14
6030 Bottom	12.7 x 38.1	Kynol	5	150	6.47
0.6 mg Pt/cm^2 rolled electrodes 45% PTFE					
6974 Top	12.7 x 38.1	Kynol	5	150	4.15
6969 Bottom	12.7 x 38.1	Kynol	5	150	3.60
0.5 mg Pt/cm^2 rolled electrodes 40% PTFE					
X017 Top	1261 cm^2	Kynol	5	150	4.58
X015 Top	1261 cm^2	Kynol	5	150	3.32
0.9 mg Pt/cm^2 rolled electrodes 40% PTFE					
X022	1277 cm^2	Kynol	5	150	6.29
X025	1277 cm^2	Kynol	5	150	5.07

- Development of an Acid Inventory Control Member

A new, more controllable spray gun has been obtained and a number of carbon paper backings have been sprayed with FEP and TFE through a metal grid in order to produce the selectively wetproofed areas desired. The problem is to spray the wetproofing material with sufficient force to penetrate the backing completely and in sufficient volume to effectively wetproof the desired areas, but not in a quantity great enough to spread out laterally through the backing causing complete wetproofing. To solve this problem, a series of backings are being sprayed under varying conditions of air and fluid mix, air pressure, and concentration of wetproofing material. TFE 3416 was chosen as the first material to be tried because of the low percentage of wetting agent it contains (0.8%) compared to most fluoromer emulsions. The wetting agent is necessary to prevent the submicron-sized particles from coagulating and precipitating out of the dispersion. However the wetting agent is also responsible for the tendency of the material to spread out in all directions. The first attempt at selectively wetproofing a backing with TFE 3416 produced fairly good results, but the nozzle of the spray gun clogged with TFE, apparently coagulated by the shear forces experienced in going through the nozzle. For this reason, work was continued with another material, FEP 120, which has not presented coagulation problems.

Several different perforated plates are being used to produce AICMs. Their hole diameters and the percentage of the total area which would be wetproofed (and available for gas flow) are listed in Table I.5 below.

TABLE I.5 COMPARISON OF PERFORATED SCREENS FOR AICM PRODUCTION

Screen	Hole Diameter, inch	% Area Wetproofed
1	3/16	50.0
2	1/8	40.5
3	1/16	29.0

Should the wetproofed areas listed in the table prove to be inadequate, the screens could be used in combination or screens with other hole sizes and patterns could be obtained. Figure I.7 shows the acid pick-up curves of an AICM backing (9C) produced with Screen #1. The backing had a 9% total FEP pick-up (i.e., including the FEP on the completely covered gas side). Although this is low, it was felt that a 9% FEP pick-up might be tolerable since Cell #1278 ran for more than 3500 hours with only 20% FEP in its anode backing. A section of this backing was combined with a 0.3 mg Pt/cm^2 catalyst layer to form an electrode. The electrode was at first inadvertently sintered at 340°C and then re-sintered at 365°C. Samples of both were also tested for acid pick-up. Cell #1341 was built with the re-sintered AICM anode and its performance indicates that it is probably flooded.

Another possible way to produce an AICM is to reduce the amount of FEP in the backing, resulting in a partial flooding of the entire backing. Cell #1278 (Table I.1) contained an anode backing with 20% FEP and Cell #1316 contained an anode backing with 28% FEP. Neither of these cells was built with pre-filled electrodes, but it was intended that the backings should pick up acid during the operation of the cell. Cell #1278 demonstrates that cells can run well with a low percentage of FEP in their anode backings, but it has not been proven whether the anode runs well despite being partially flooded, or if the low percentage of FEP is sufficient to prevent flooding of the anode backing. If the backing is, in fact, partially flooded, then using a low FEP backing for the anode presents an easy, reproducible way of preparing AICMs. If the backing is not partially flooded, then it will be necessary to produce selectively wetproofed anode backings to provide the needed capacity for electrolyte volume change. This technique, although promising, has not yet been successfully demonstrated.

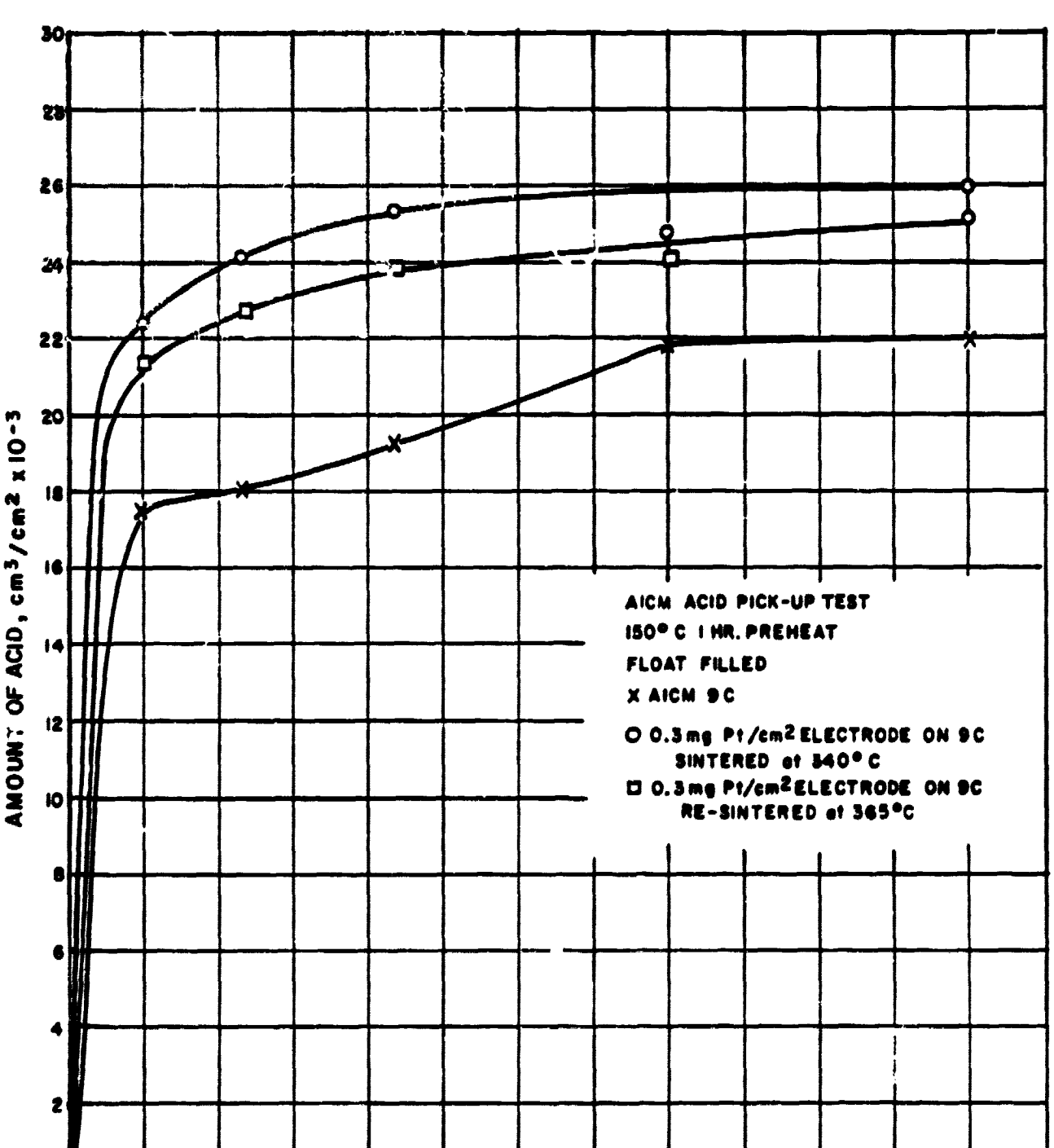

FIGURE I.7 AICM ACID PICK-UP IN BACKING PAPERS WITH ELAPSED TIME

1.4 Bipolar Plate Technology

- Bipolar Plate Molding

Fifteen 480 cm^2 bipolar plates were fabricated with 67% A-99 graphite/33% Varcum 24-655. These plates meet current specifications and will be used in future stack performance tests. Plates were fabricated with 75% A-99 graphite/25% Varcum 24-655 for 25 cm^2 cells and are retaining their integrity after ~ 2000 hours of cell testing.

- Carbonization

Samples of graphite/resin composites were heated to approximately 900°C in a nitrogen atmosphere over a six day period. A programmable temperature controller varied the heating rate during this period.

During carbonization, sections of 13 cm x 38 cm x 0.40 cm bipolar plates did not blister, but the thicker 10 cm x 10 cm x 0.55 cm plates blistered severely. The heating cycle and the length of the heating cycle will depend on the thickness of the parts. Future carbonization runs will involve locating the region of the heating cycle where blistering occurs for the thicker parts, and then adjusting the heating rate in that region.

Bipolar plates will warp during carbonization unless restrained. Weights (exerting pressure, 4.5 Pa) placed on plates in Run #2 reduced the amount of warping from that observed in Run #1. The borders of the plates used for sealing the cells is thicker than the interior ribbed portion of the plates. To uniformly distribute the load over the plates, shims will be used in future tests.

Figures I.8 and I.9 show the percentage change in linear dimensions as a function of the resin content. According to the figures, no significant differences between colloid and Varcum exist. This information will be of value in designing fuel cells with carbonized parts.

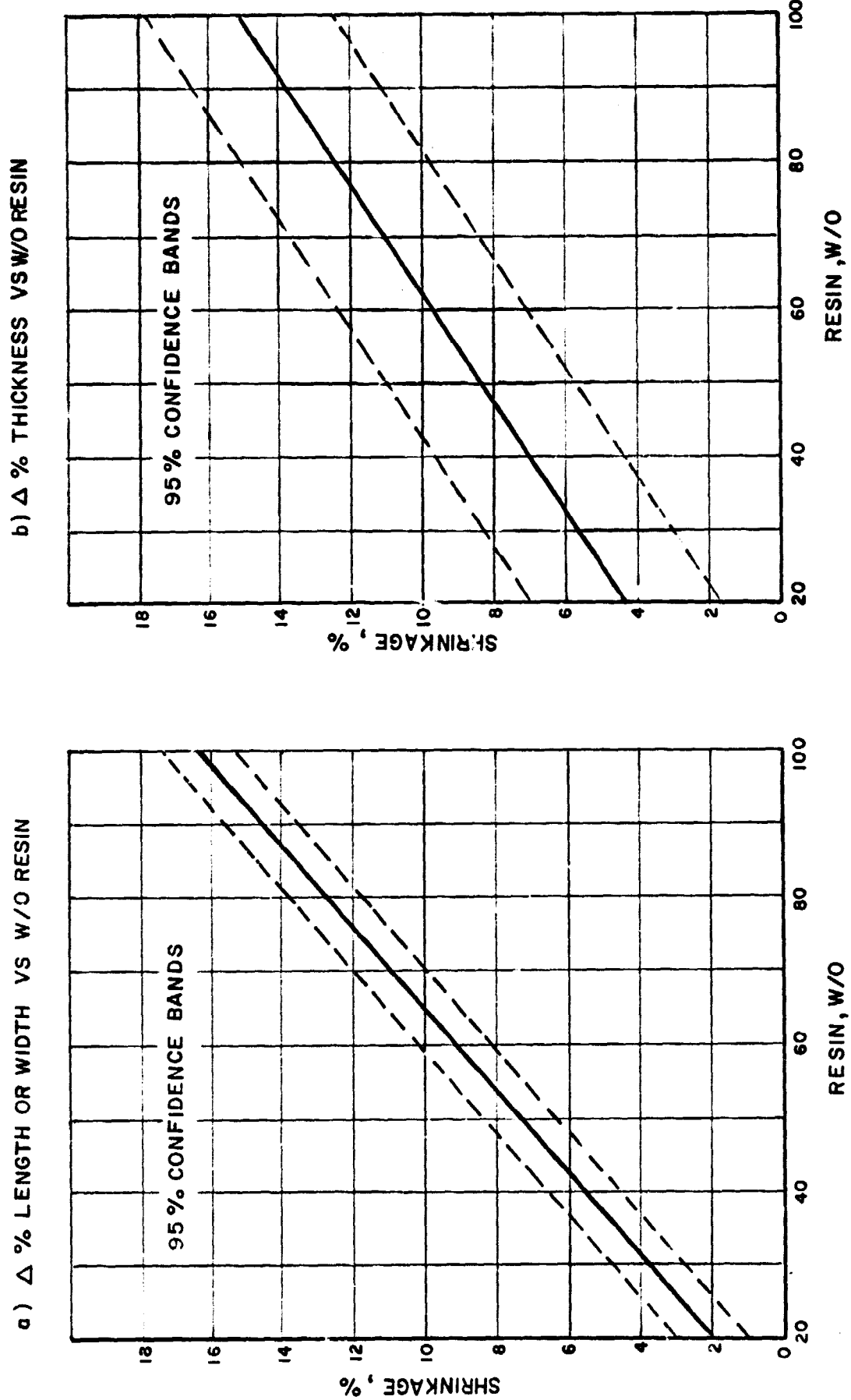

FIGURE I.8 SHRINKAGE IN CARBONIZED GRAPHITE/COLLOID 8440 RESIN

D0697

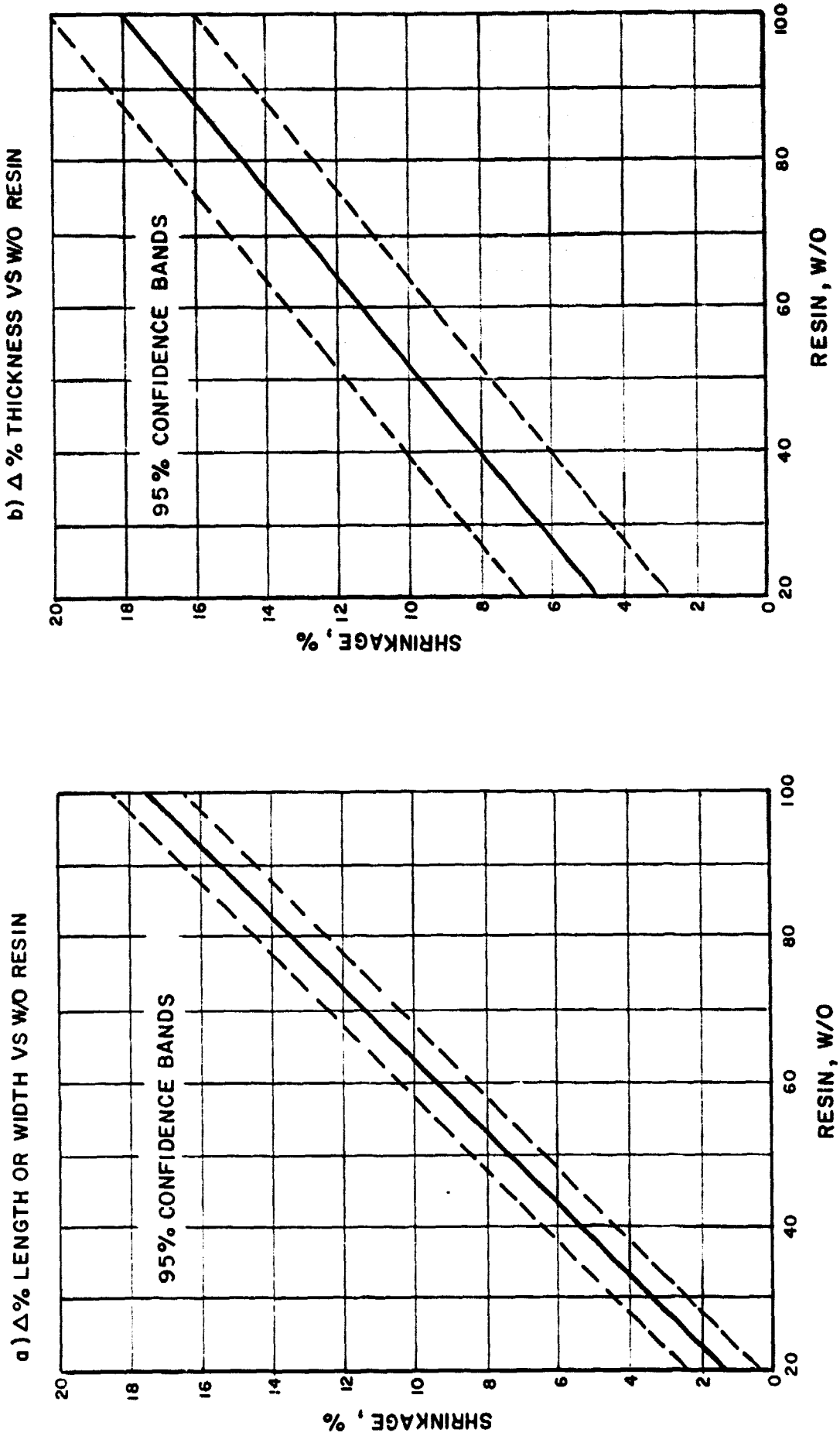

FIGURE I.9 SHRINKAGE IN CARBONIZED GRAPHITE/VARCUM 24-655 RESIN

D0698

TASK II. MATERIAL EVALUATION

2.1 Component Corrosion Resistance

A study of the effects of 185°C concentrated phosphoric acid on bipolar plate materials is currently in progress. The following effects may occur with the samples in test: corrosion, surface etching, acid absorption, thickness changes, and absorption of moisture from atmospheric air after exposure to phosphoric acid. To evaluate possible candidate materials for bipolar plates, all the above factors should be taken into consideration and their significance determined.

Samples were placed in 185°C ∿100% phosphoric acid. Periodically the samples were removed from the acid and immersed in water, then dried, weighed and measured for thickness. This method of measuring weight and thickness changes will be referred to as "Method I". A second method, "Method II", was to boil the samples in deionized water after removal from the acid, and then weigh and measure thickness. For the selected samples, absorption of moisture from atmospheric air after acid exposure was investigated to determine possible sources of error in the weight measurements. Also microscopic examination of most samples showed surface etching.

Figure II.1 shows the weight changes observed for two Varcum 24-655 samples. To describe the determination of the parameters listed above, the schematic in Figure II.2 will be used. Line AB, which can be determined by least squares linear regression, shows the weight changes due to phosphoric acid exposure observed using Method I. Line BC shows the absorption of moisture after acid exposure. The removal of acid by boiling is shown by line CD. The actual amount of acid absorbed during exposure to H_3PO_4 would be the weight change in line segment CD minus the weight change in line segment BC if all the acid was removed during boiling. Figure II.3 illustrates weight loss due to desorption

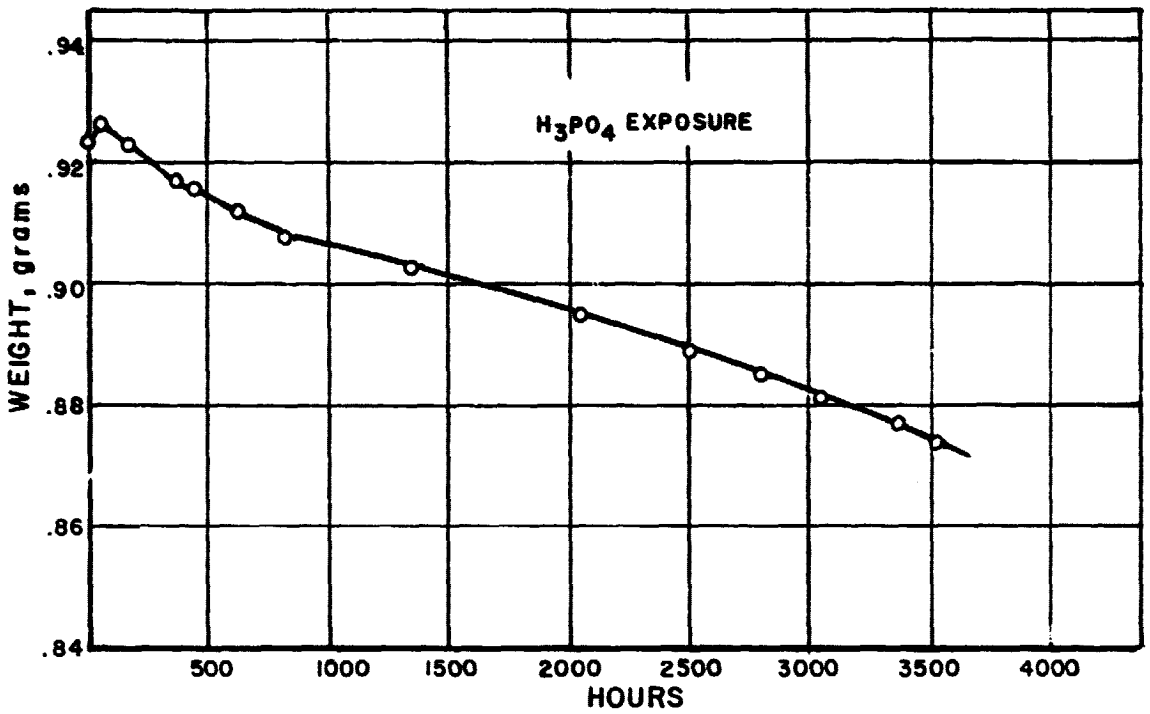

a) 100% VARCUM 24-655, SAMPLE 431A

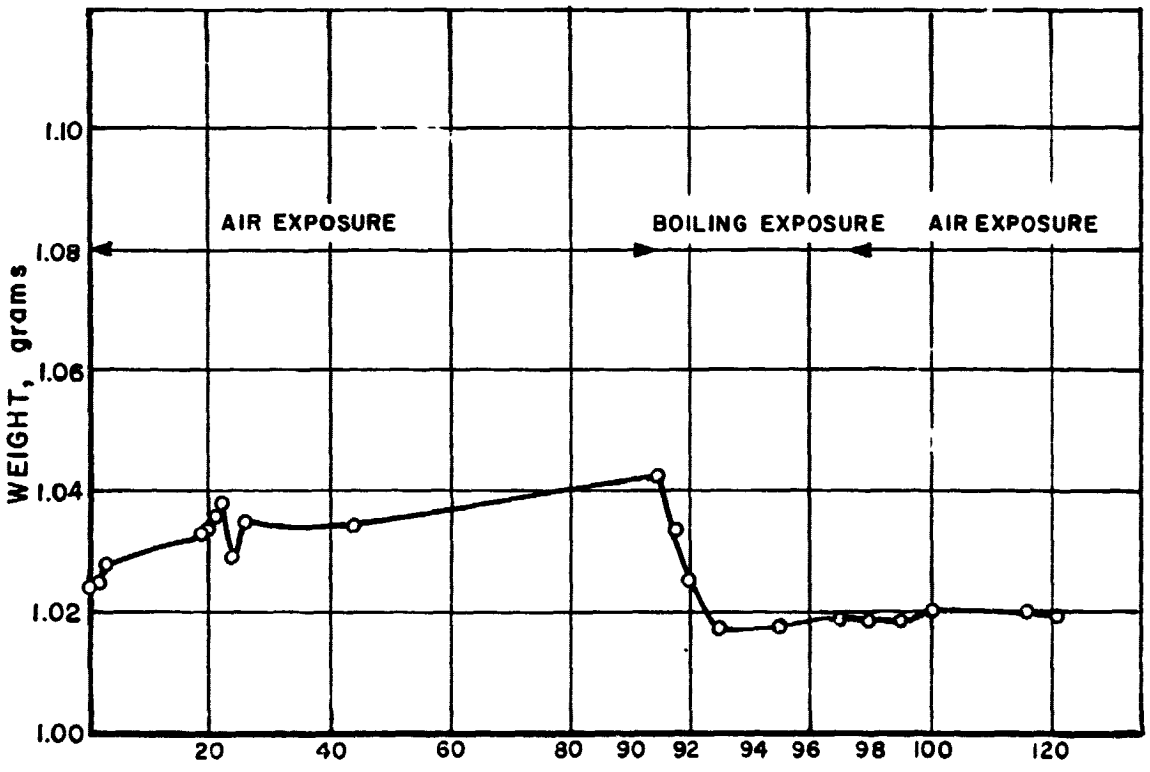

b) 68% GRAPHITE / 32% VARCUM 24-655, SAMPLE 396A

FIGURE II.1. WEIGHT CHANGES DURING AND AFTER H_3PO_4 EXPOSURE

D0900

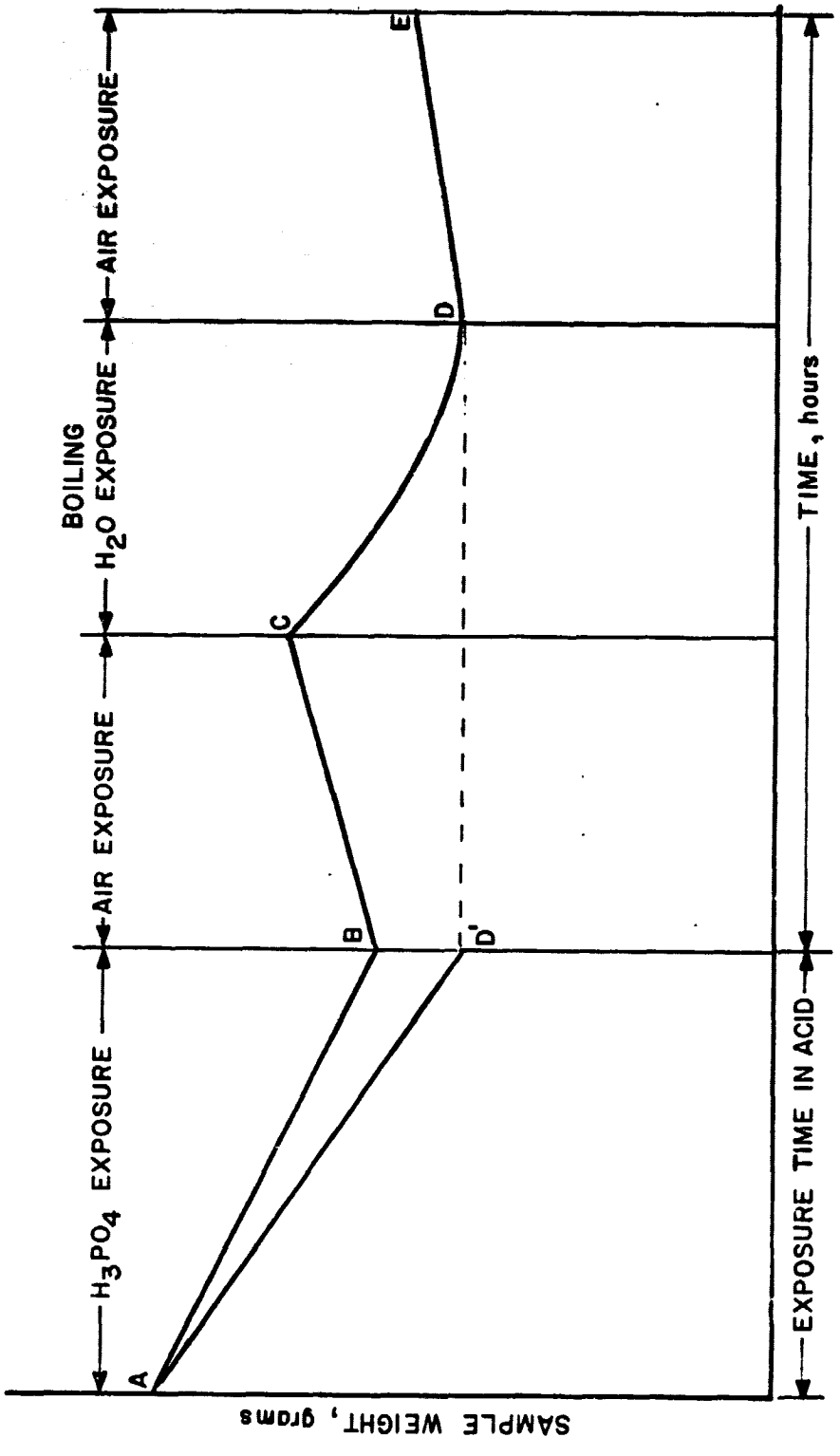

* WEIGHT CHANGES IN MILLIGRAMS

FIGURE II.2 OBSERVABLE WEIGHT CHANGES IN GRAPHITE/RESIN

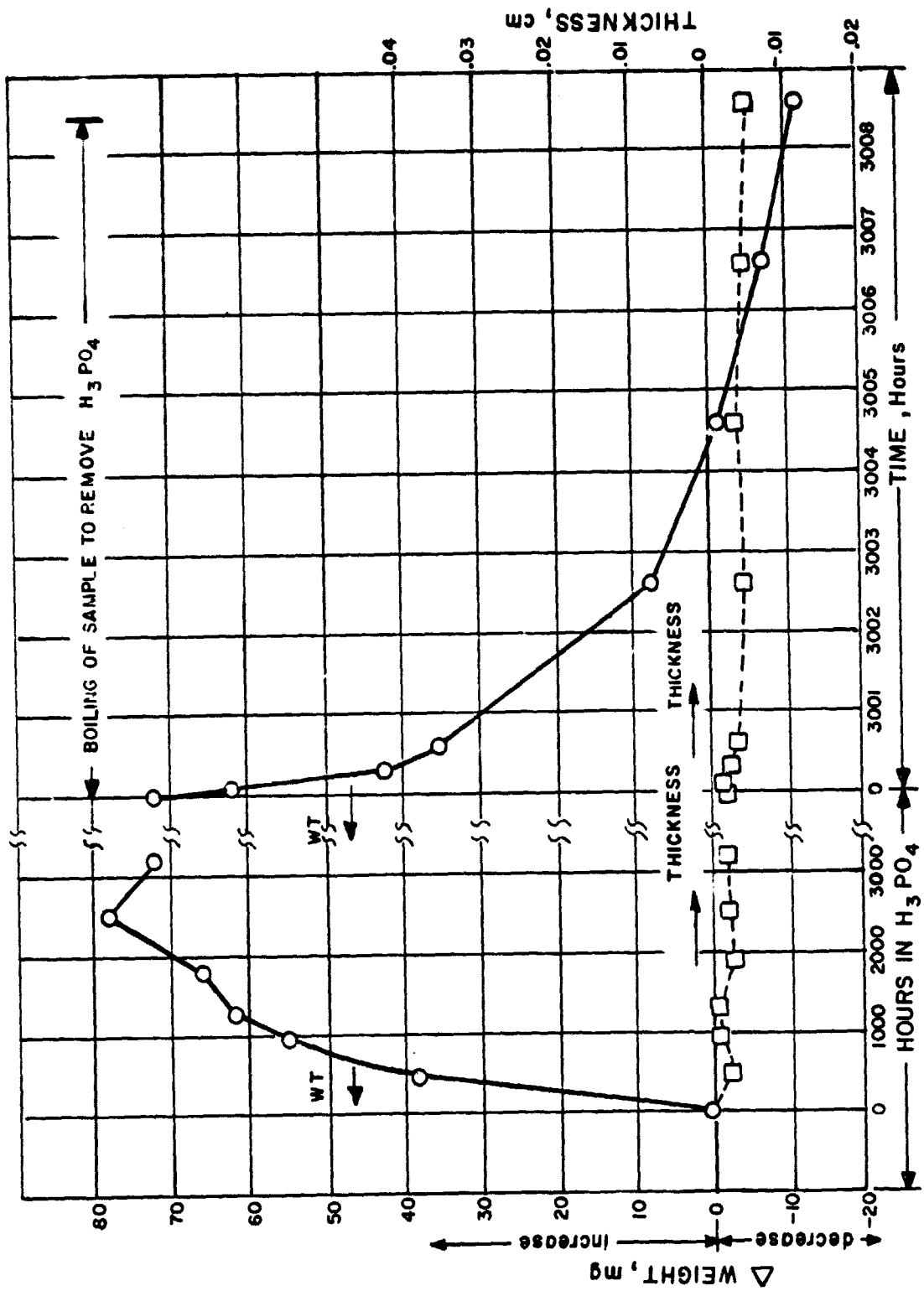

FIGURE II.3. ACID CORROSION OF 68% GRAPHITE/32% COLLOID 8440 (SAMPLE #389A IN 180°C H_3PO_4)

D0901

of acid for over 8 hours. The pH of boiled water was still acidic. Line DE of Figure II.2 shows the amount of moisture absorbed from atmospheric air after boiling, indicating the amount of acid remaining in the sample. A corrosion rate is calculated from the slope of line AD[1] by using a sample surface area calculated from the initial weight, density and thickness. This is an apparent corrosion rate because all the acid may not be removed from the samples.

Scanning electron microscopy of 100% phenolic resin samples shows a surface not exposed to the acid (Figure II.4) and also reveals etching of surfaces due to acid exposure (Figures II.5 and II.6). From these SEM photographs, the grain size of the surface etching can be measured.

Thickness measurements as shown in Table II.1 were taken along with weight measurements.

2.2 Physical Property Measurements

The resistivity of graphite/resin composites with Varcum 24-655 and Colloid 8440 resin were calculated. Previously measured graphite/resin composites contained A-99 Asbury graphite (particle size 17 μm). The effect of the addition of Asbury 850 graphite on the resistivity was investigated. The same four-point method which eliminates the effects of contact resistance was used to measure the voltage drop across machined round samples. The resistivity of the samples was measured perpendicular to pressing. As shown in Table II.2, the addition of Asbury 850 (particle size 0.05 to 0.06 μm) increased the resistivity. Originally, Asbury 850 was added to the graphite mixture to improve its flow behaviour. The recent results with increased resistivity suggest a fresh look at this mixture.

2.3 Estimation of Cell Component Resistance

Table II.3 shows the estimated resistance of cell components. The contact resistance seems to be a major factor in the cell IR. The contact resistance between backing paper and bipolar plate

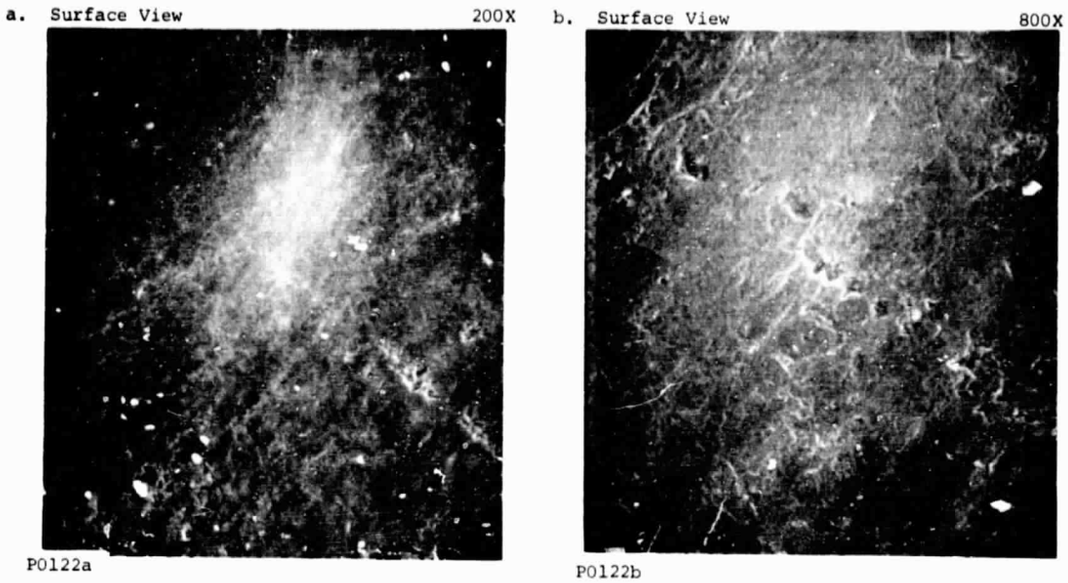

FIGURE II.4 SEMS OF 100% COLLOID 8440 RESIN WITH NO ACID EXPOSURF (Sample 357-03)

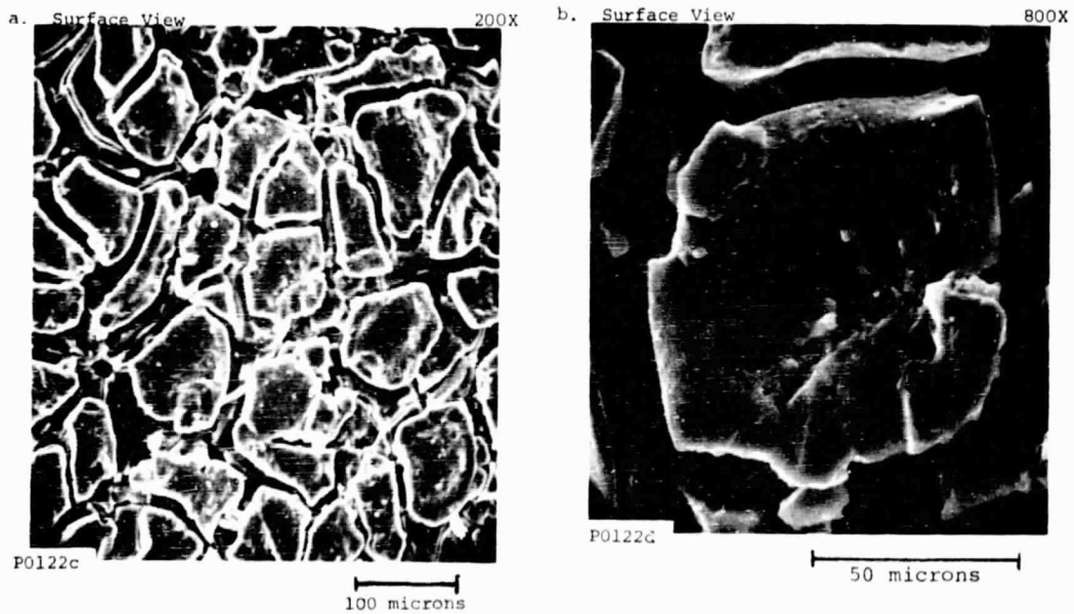

FIGURE II.5 SEMS OF 100% COLLOID 8440 RESIN AFTER 1500 HOURS OF 185°C H_3PO_4 EXPOSURE (Sample 357-A)

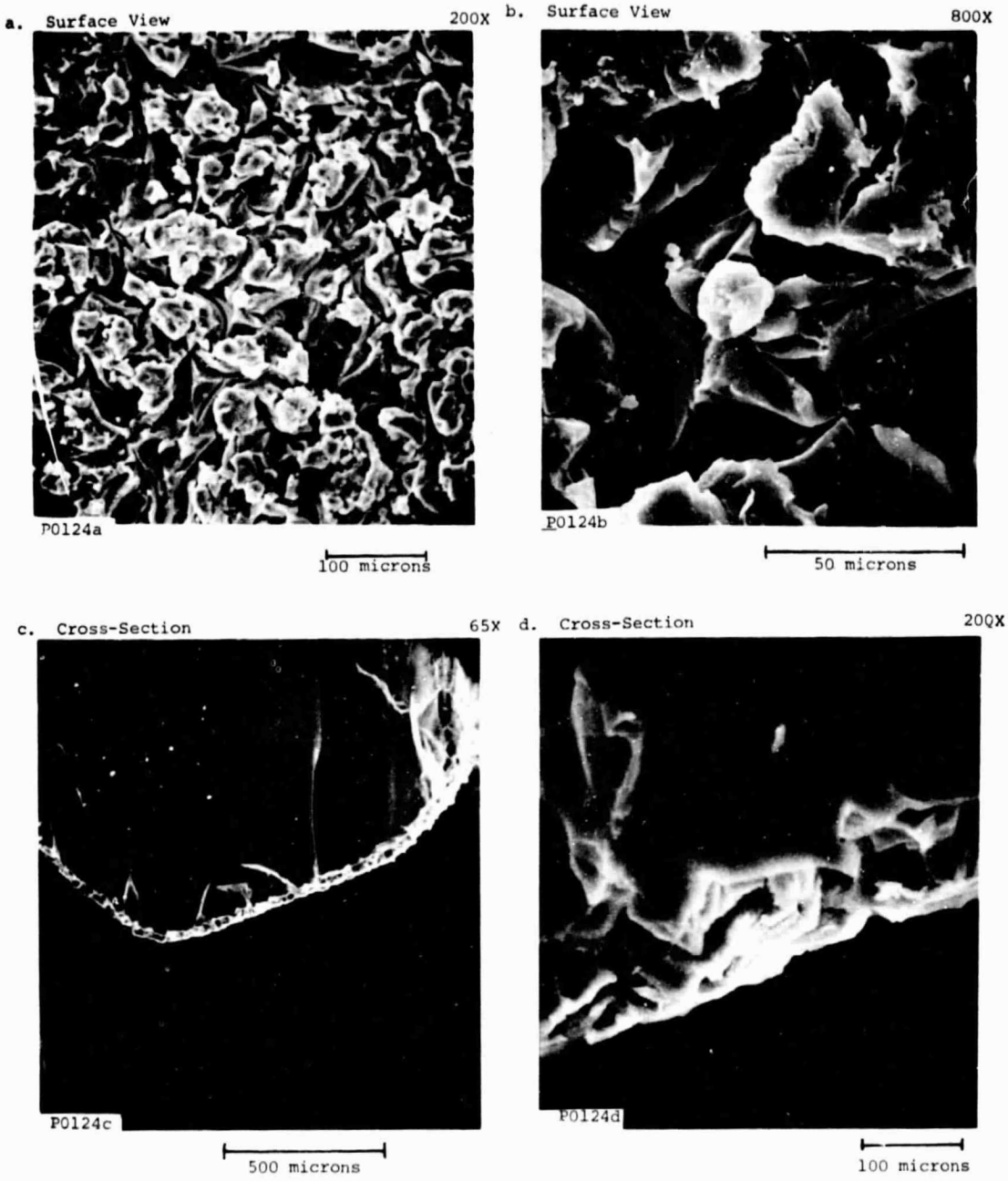

FIGURE II.6 SEMS OF 100% VARCUM 24-655 RESIN AFTER 2250 HOURS OF 185°C H_3PO_4 EXPOSURE (Sample 349-1B)

TABLE II.1 COMPONENT CORROSION RESISTANCE TO 185°C H_3PO_4

Resin	Sample Composition w/o Graphite / w/o Resin	Sample #	Hours in H_3PO_4	Δ Weight, mg	Δ Thickness, cm	Minimum Corrosion Rate, $\mu g/hr/cm^2$	Minimum Acid Absorption, mg	Adsorption of H_2O From Air in 24 Hrs, mg	Surface Etching Grain Size cm x 10^2
COLLOID 6440	0/100	397A	0	Control Sample	-	0	0	3	-
	0/100	397B	3072	+14.4	-.0003	0.38	26	-	1 to 3
	0/100	430A	3123	+25.3	+.0031	1.36	100	-	1.0 to 1.5
	0/100	430C	2643	+49.7	+.0066	0.60	75	29	-
	78/22	387A	3861	+10.0	+.0124	4.38	90	23	-
	68/32	389A	3555	+39.9	-.0033	0.60	84	-	-
	68/32	386A	3828	+56.7	+.0091	0.55	10	31	-
	67/33	161A	2069	+86.0	+.0056	-	57	-	-
VARCUM 24-655	0/100	349C	1740	-28.7	-.0012	1.07	0	-	0.5
	0/100	431A	3533	-49.3	-.0020	1.42	2	1	-
	78/22	394A	1874	-13.0	-.0009	12.22	23	-	-
	68/32	396A	3842	-13.0	+.0015	3.14	18	5	-
	68/32	405A	3276	-17.8	-.0013	0.43	16	-	-
H-RESIN H-A43	0/100	346C	2354	-49.5	-.0048	2.75	1	-	-
	68/32	390A	3787	-11.7	-.0023	.21	1	-	-
PLENCO 956	0/100	373C	2354	-13.4	-.0041	.74	-1	-	-
PLENCO 402	0/100	374C	2354	-22.2	+.0015	.71	0	-	-
XYLOK 225	-	375B	2354	-40.0	-.0018	1.25	3	-	-
VARCUM 29319	0/100	356-1	1248	+ 1.4	-.0007	-	-	-	-
VARCUM 29703	0/100	355-1	2151	-26.0	-.0009	-	-	-	0.5
RADEL	0/100	5010-3	3694	+ 3.5	-.0018	-	-	-	-
(POLYPHENYLSULFONE)	0/100	RADEL-C	1956	- 3.0	+.0025	-	-	-	-
POLYSULFONE	0/100	UDEL-A	1885	- 6.0	+.0538	-	-	-	-
	0/100	UDEL-B	1885	- 9.0	+.0467	-	-	-	-
POLYMETHYLPENTENE	0/100	PMP-A	725	- 5.0	+.0076	-	-	-	-
	0/100	PMP-B	517	- 6.0	+.0046	-	-	-	-
POLYETHERSULFONE	0/100	Victrex 300P-1	636	-16.0	+.0020	-	-	-	-
	0/100	Victrex 600P-1	636	-14.0	+.0030	-	-	-	-

TABLE II.2 INCREASE IN RESISTIVITY OF GRAPHITE/RESIN WITH ADDITION OF ASBURY 850 GRAPHITE

Resin	Composition w/o Graphite / w/o Resin	Resistivity, Ω-cm	
		100% A-99 Graphite	73% A-99/27% 850 Graphite
COLLOID 8440	78/22	.009	.011
	78/22	.009	.011
	72/28	.014	-
	72/28	.014	-
	68/32	.026	.046
	68/32	.022	.052
	68/32	.019	-
	67/33	-	.060
VARCUM 24-655	78/22	.007	.010
	78/22	.007	.010
	72/28	.012	-
	68/32	.019	.032
	68/32	.017	-
	68/32	.016	-

TABLE II.3

ESTIMATED RESISTANCE OF CELL COMPONENTS

(12.7 cm x 38.1 cm [5 in. x 15 in.] Stack)

Component	Room Temperature Resistance* (mΩ)	Remarks†
Stackpole Backing Paper in C-C Plate (No FEP)	0.01	Resistivity$^{\circ}$ = 0.0834 ohm-cm Thickness = 0.0348 cm
Stackpole Backing with 33.3% FEP in C-C Plate	0.02	Resistivity$^{\circ}$ = 0.146 ohm-cm Thickness = 0.0345 cm
C-C Plate with 33% Colloid**	0.17	Resistivity†† = 90 mΩ-cm
Contact of Backings on Cathode and Anode Ribs of C-C Plate of 33% Colloid	0.15	33.3% FEP in Backing
Contact Between Silver Plate Terminal and Backing Plus Contact Between Backing and C-C Plate Ribs	0.14	33% C-C Plates 33.3% FEP in Backing
A-B Plate with 33% Colloid	0.17	Resistivity†† = 90 mΩ-cm
A-B Plate with 25% Colloid	0.10	Resistivity†† = 40 mΩ-cm
Contact of Backings on Cathode and Anode Ribs of A-B Plate of 33% Colloid	0.16	33.3% FEP in Backing
Contact of Backings on Cathode and Anode Ribs of A-B Plate of 25% Colloid	0.20	33.3% FEP in Backing
Composite of Backing Paper with 15.6% FEP and Electrode	0.02	Pt Loading = 0.4 mg/cm^2
Composite of Backing Paper with 38.5% FEP and Electrode	0.04	Pt Loading = 0.3 mg/cm^2 40% Vulcan
Electrolyte in Kynol Matrix	0.74	100% Acid at 40°C Resistivity = 12.5 ohm-cm Thickness = 0.047 cm Void Fraction = 0.86

* Based on active area = 387 cm^2
Compression = 90 psia

† Details of calculations are given in Appendix A.

** Use of slightly different dimensional samples may show slight discrepancy in values reported elsewhere.

° From stack pile measurement.

†† Four point measurement in planar direction, estimated in the axial direction.

could be reduced about half for a C-C type bipolar plate after cleaning the rib surfaces with the finest grade sandpaper. For this reason the plates are always cleaned in the actual cell. The resistance of C-C and A-B type plates with 33% Colloid are very close to each other, as shown in the table. Total estimated resistance of a 12.7 cm x 38 cm (5 in. x 15 in.) stack of 3 cells with A-B plates is 3.8 mΩ at room temperature while measured cell resistance is 4.5 to 6 mΩ at 177°C. We expect the resistance of a cell stack to decrease as temperature is increased. Further investigation will be performed to determine component resistance at elevated temperatures so that the total stack resistance can be predicted and compared with the measured values.

TASK III. ENDURANCE TESTING

3.1 Prediction of P_4O_{10} Vapor Concentration

In the previous quarter, vapor-liquid equilibrium data* in the temperature range of 188 to 302°C was used with van Laar and Wilson equations to predict P_4O_{10} vapor concentrations. It was found that the use of equilibrium data at higher temperatures leads to predictions closer to the experimental data** This was attributed to the potentially better accuracy of equilibrium data at higher temperatures. This quarter, equilibrium data in the higher temperature range (302 to 370°C) was used to see if the predicted values remained constant. The predicted P_4O_{10} vapor concentrations are listed in Table III.1. It was observed that the P_4O_{10} concentration continuously decreased with temperature. The predicted concentrations were lower (0.09 to 0.36 ppm) than the experimental value, except in the case of the Wilson equation where equilibrium data at 335°C was used (0.69 ppm). This made it impossible to choose a reliable set of parameters for reasonably good predictions.

The best parameter values can be obtained by regression analysis of the experimental data $\left(G^E/RT - V\Delta\ X_1\right)$ relationship at constant temperature†. G^E represents the excess Gibbs free energy. The goodness of fit depends upon the suitability of the type of equation used. If a plot of $G^E/x_1x_2RT\ V\Delta\ x_1$ were linear, Margules equation would provide a good fit. If a plot of x_1x_2RT/G^E is linear, the van Laar equation would provide a good fit. If neither plot is linear, the Wilson equation might work or a more complicated equation is required.

---

* Brown, E. H., Whitt, C.D., "Vapor Pressure of Phosphoric Acids," Ind. & Eng. Chem., 44, No. 3, pp 615 (March 1952).

** United Technologies, Power Systems Division, South Windsor, CT, "Improvement of Fuel Cell Technology Base", Technical Progress Report No. 3, prepared for U.S. Dept. of Energy under Contract ET-76-C-03-1169, June 1978.

† Smith, J.M., Van Ness, H.C., "Introduction to Chem. Eng. Thermodynamics," Third Edition, McGraw-Hill Book Co., pp 335, 1975.

TABLE III.1

P_4O_{10} CONCENTRATION PREDICTED USING EQUILIBRIUM DATA (302 to 370°C Range)

Equation	Temperature*, °C	Vapor Pressure of Pure P_4O_{10} (Solid H Form) $10^4 n/m^2$, mm Hg	Parameters		Predicted P_4O_{10} Vapor Concentration @ 191°C, 99.5 wt% acid, ppm by vol.
			a	b	
van Laar	335	4.77 (357.7)	-170.0	-6.68	0.31
	370	13.27 (994.9)	-165.5	-7.39	0.09
			c_3	c_4	
Wilson	335	4.77 (357.7)	1.5799	1468.0	0.69
	370	13.27 (994.9)	3.2812	2040.5	0.36

* Temperature at which experimental vapor-liquid equilibrium was measured by Brown and Whitt, cited.

The computation of G^E, however, requires the knowledge of solubility parameters and molar liquid volumes for the P_4O_{10}-H_2O system. Since the above properties are not available in the literature, a regression analysis cannot be performed.

A new correlation* was applied to extrapolate the vapor-liquid equilibrium data at normal boiling points (N.B.Pt)** to a temperature range of 163 to 218°C (covering the fuel cell operating temperature range). The correlation is

$$T \log \nu = \text{constant}$$

where,

T is temperature

ν is the activity coefficient in the liquid phase.

This correlation has helped in estimating the variation of ν values with temperature but it is approximate. The predicted values of P_4O_{10} vapor concentration as a function of temperature using this equation are plotted at various acid concentrations (covering the range of interest) in Figure III.1.

As expected, the P_4O_{10} vapor concentration increased with temperature and acid concentration. The effect of temperature was stronger than that of acid concentration. The P_4O_{10} vapor concentration predicted at 191°C varied from 0.73 to 1.02 ppm for the acid concentration range selected. The predicted concentrations are compared with the experimental values in Table III.2.

3.2 Measurement of P_4O_{10} Vapor Concentration

Two more experiments (2 and 3) were conducted to duplicate the results of the previous experiment. The duration of the

---

* Perry, R.H., Chilton, C.K., and Kirkpatrick, S.D., Editors, "Distillation", Chemical Engineers Handbook, Fourth Edition, 1963, pp 13-8.

** Brown, E.H. and Whitt, C.D., op cit, pp 615.

ENERGY RESEARCH CORPORATION

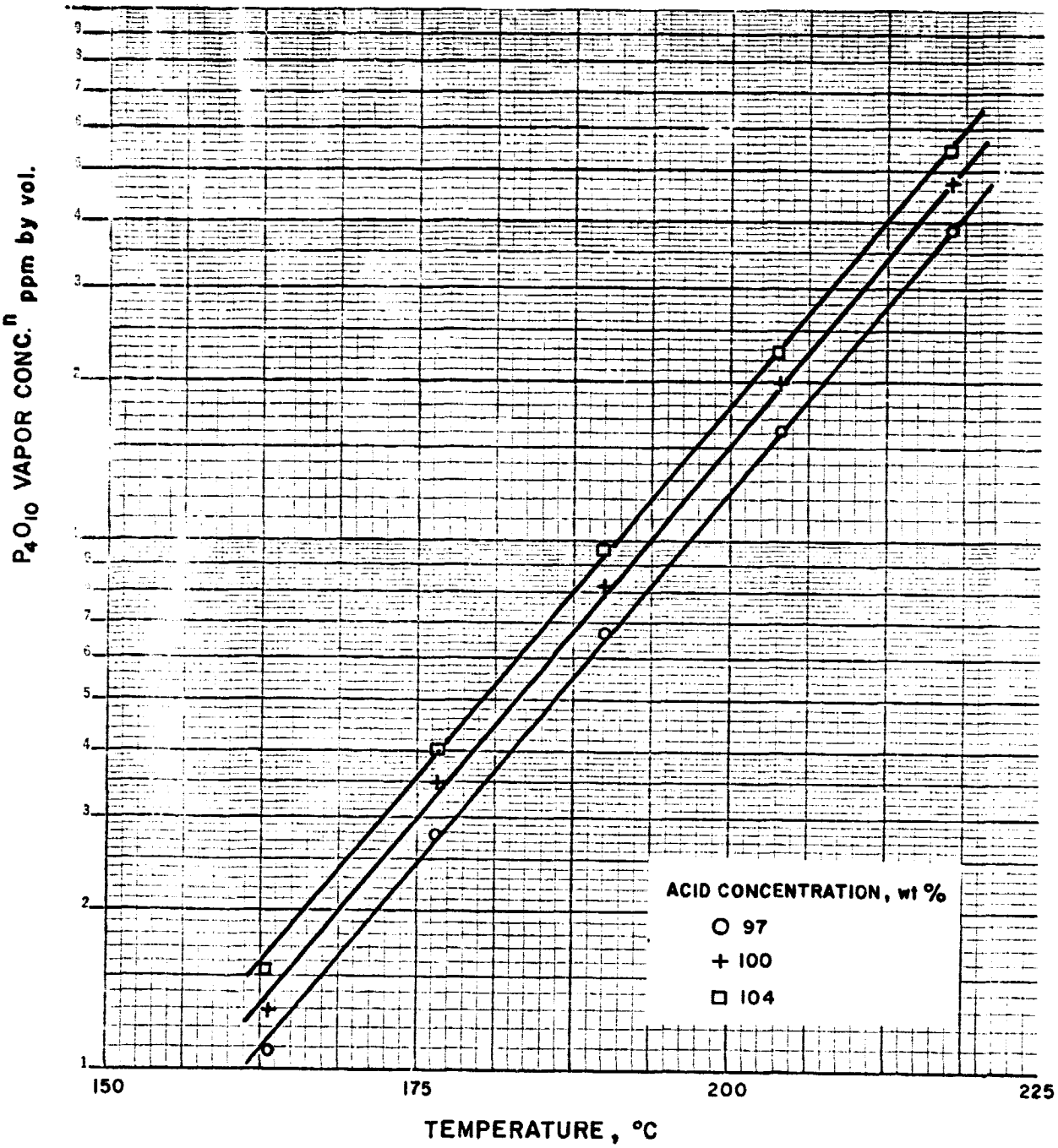

FIGURE III.1 P_4O_{10} VAPOR CONCENTRATION PREDICTED BY $T \ln v$ = CONSTANT

TABLE III.2

P_4O_{10} CONCENTRATIONS EXTRAPOLATED FROM NORMAL BOILING POINT DATA

Acid Concentration, Wt%	Predicted P_4O_{10} Vapor Concentration, ppm by volume	Comments
97	0.73	-
100	0.90	UTC data 0.46 ppm @ 99.5 wt% acid
104	1.02	ERC data @ 103.3 wt% acid expt 1: 2.0 ppm expt 2: 0.7 ppm expt 3: 1.0 ppm

experiments was approximately 340 hours. In Experiment 3, platinum black electrodes were used to eliminate the weight changes due to possible carbon corrosion. The results of the experiments are compared with the previous experiment in Table III.3. The acid concentration in the cell during operation was estimated to be 103.3 wt%. The lower loss obtained in Experiment 2 may be partially due to leakage of air from the edges and crossleakage in the cell. This edge leakage was avoided in Experiment 3. The P_4O_{10} vapor concentration obtained from the component weight analysis in Experiment 3 (1.0 ppm) was in close agreement with the predicted value reported in Table III.2. The low P_4O_{10} vapor concentrations obtained from adsorber weight analysis in all cases indicated that the assumption of $Fe_3(PO_4)_2$ formation was invalid.

A new experiment has been started to measure the P_4O_{10} vapor concentration at 191°C with different acid concentrations. The air is humidified in two steps, to a dew point of 71°C, so as to yield an equilibrium acid concentration of about 98%.

3.3 Effect of Operating Variables on Cell Performance

Testing of 350 cm^2 stacks for this quarter is summarized in Table III.4. Several stacks (12.7 cm x 38.1 cm) have been assembled for different testing purposes.

3.3.1 Effect of Compression on the Stack

Ohmic resistance of Stack 376 at OCV as a function of applied compression was reported in the last quarter. Additional experiments have been conducted to study the effect of compression on resistance as well as on crushing of the backing paper.

Stack 378 was assembled using the same plates as Stack 376 but with reduced shims. The stack was torqued in a step-by-step manner. The ohmic resistance of the stack at 40A (112 mA/cm^2)

TABLE III.3

MEASURED P_4O_{10} VAPOR CONCENTRATIONS

		Experiment 1	Experiment 2	Experiment 3
% of the original acid removed		95	18	30
P_4O_{10} vapor concentration @ 191°C and 103.3 wt% acid, ppm by vol.	From component wt. measurements	2.0	0.7	1.0

TABLE III.4 STACK TESTING SUMMARY

- Active Testing Update
- 108 ASF (40 A)

STACK NO.	347	349	351	352
TEST OBJECTIVE	HUMIDIFICATION, FREEZING ENDURANCE	HIGH CURRENT DENSITY ENDURANCE	SiC MATRIX	SRF TESTING, HUMIDIFICATION
NO. CELLS	3	3	3	3
ANODE mg Pt/cm^2	.58 .61 .55	.54 .58 .55	.29 .32 .26	.28 .29 .27
CATHODE mg Pt/cm^2	.87 .89 .96	.94 .96 .90	.53 .49 .62	.62 .61 .64
MATRIX	KYNOL	KYNOL	SiC	KYNOL
PLATES/CONDITION	FAIR	FAIR	GOOD	GOOD
PEAK PERFORMANCE (Volts) Air-	.59 .62 .61	.61 .62 .63	.58 .61 .58	.60 .60 .60
PEAK PERFORMANCE (Volts) OCV-	.84 .84 .84	.80 .81 .82	.72 .80 .72	.84 .84 .84
PRESENT PERFORMANCE (Volts) Air-		.58 .61 .59		
PRESENT PERFORMANCE (Volts) OCV-		.77 .82 .84		
O_2 GAIN (Volts)		.08 .08 .08		
INITIAL mΩ READING	5.6	4.4	4.1	4.8
ACID HISTORY, hrs		NO ACID SINCE 3609		
GAS UTILIZATION/ SENSITIVITY		H_2 SENSITIVE		
TOTAL HOURS	LIFE - 4043 FREEZER - 730 CYCLES - 10	LIFE - 5365 H.C.D. - 4263	2106	4009
REMARKS	DISASSEMBLED		DISASSEMBLED	DISASSEMBLED

TABLE III.4 STACK TESTING SUMMARY

- Active Testing Update
- 108 ASF (40 A)

STACK NO.	357	363	366	367
TEST OBJECTIVE	SEAMED ELECTRODES	45% TFE ELECTRODES	50% TFE CATHODE CATALYST	45% TFE CATHODE
NO. CELLS	3	3	3	3
ANODE mg Pt/cm^2	.57 .57 .60	.54 .66 .63	.26 .26 .24	.31 .19 .30
CATHODE mg Pt/cm^2	.90 .92 .94	.64 .59 .60	.58 .58 .62	.56 .48 .52
MATRIX	KYNOL	KYNOL	KYNOL	KYNOL
PLATES/CONDITION	GOOD	GOOD	FAIR	GOOD
PEAK PERFORMANCE (Volts) Air-	.60 .57 .63	.56 .57 .54	.58 .60 .57	.59 .60 .60
PEAK PERFORMANCE (Volts) OCV-	.84 .74 .88	.82 .82 .77	.83 .85 .82	.83 .83 .83
PRESENT PERFORMANCE (Volts) Air-				
PRESENT PERFORMANCE (Volts) OCV-				
O_2 GAIN (Volts)				
INITIAL mΩ READING	4.9	6.2	5.4	5.3
ACID HISTORY, hrs		ACID ADDED 2724	ACID ADDED 2741	
GAS UTILIZATION/ SENSITIVITY		VERY AIR AND H_2 SENSITIVE	AIR & H_2 SENSITIVE	
TOTAL HOURS	2998	3176	2837	1902
REMARKS	DISASSEMBLED	SCHEDULED FOR TERMINATION		DISASSEMBLED

TABLE III.4 STACK TESTING SUMMARY

- Active Testing Update
- 108 ASF (40 A)

STACK NO.	368	369	377	378
TEST OBJECTIVE	HUMIDIFICATION, NO END PLATE SEALS	SRF ENDURANCE	SiC MATRIX, COMPRESSION	COMPRESSION
NO. CELLS	3	3	3	3
ANODE mg Pt/cm^2	.55 .56 .59	.30 .28 .30	.29 .30 .29	.32 .29 .30
CATHODE mg Pt/cm^2	.60 .59 .59	.60 .59 .59	∿ 0.6	
MATRIX	KYNOL	KYNOL	SiC	KYNOL
PLATES/CONDITION	FAIR	FAIR	GOOD	GOOD
PEAK PERFORMANCE (Volts) Air-	.57 .60 .58	.60 .61 .60	.61 .65 .60	.61 .60 .61
PEAK PERFORMANCE (Volts) OCV-	.82 .84 .84	.83 .84 .85	.76 .81 .82	.87 .87 .86
PRESENT PERFORMANCE (Volts) Air-	.54 .59 .58			
PRESENT PERFORMANCE (Volts) OCV-	.87 .89 .90			
O_2 GAIN (Volts)			.06 .06 .07	.08 .08 .08
INITIAL mΩ READING	4.9	4.7	4.3	4.7
ACID HISTORY, hrs	NO ACID SINCE 1127		ACID REPLENISHMENT WAS NOT ACHIEVED	
GAS UTILIZATION/ SENSITIVITY	AIR AND H_2 SENSITIVE			
TOTAL HOURS	LIFE TEST - 2133 HUMID - 769	LIFE TEST - 2313 SRF - 1083	121	29
REMARKS		DISASSEMBLED	DISASSEMBLED	DISASSEMBLED

TABLE III.4 STACK TESTING SUMMARY

- Active Testing Update
- 108 ASF (40 A)

STACK NO.	379	380	381	382
TEST OBJECTIVE	SHEET MOLD ELECTRODES	ENDURANCE	WET ASSEMBLY SiC MATRIX	THICK MATRIX
NO. CELLS	3	3	3	3
ANODE mg Pt/cm^2	.19 .20 .24	.35 .33 .34	.30 .32 .29	.31 .33 .29
CATHODE mg Pt/cm^2	.48 .38 .38	.57 .63 .59	.58 .58 .59	.52 .56 .55
MATRIX	KYNOL	SiC	SiC	3X KYNOL
PLATES/CONDITION	GOOD	FAIR	FAIR	GOOD
PEAK PERFORMANCE (Volts) Air-	.64 .65 .63	.63 .67 .55	.64 .63 .62	.55 .57 .52
PEAK PERFORMANCE (Volts) OCV-	.89 .89 .87	.78 .90 .70	.82 .81 .76	.88 .88 .88
PRESENT PERFORMANCE (Volts) Air-	.57 .60 .57	.63 .67 .55	.58 .62 .58	
PRESENT PERFORMANCE (Volts) OCV-	.84 .86 .84	.78 .90 .70	.73 .84 .72	
O_2 GAIN (Volts)	.09 .09 .09	.06 .05 .11	.09 .05 .08	
INITIAL mΩ READING	5.1	3.6	4.8	
ACID HISTORY, hrs	ACID ADDED 1416	ACID ADDED 886	ACID SUPPLY REMOVED 1127	
GAS UTILIZATION/ SENSITIVITY		AIR SENSITIVE		
TOTAL HOURS	1848	1167	1343	47
REMARKS	MANIFOLDS CLEANED IMPROVING	AT 100 mA/cm^2		DISASSEMBLED

TABLE III.4 STACK TESTING SUMMARY

- Active Testing Update
- 108 ASF (40 A)

STACK NO.	383	384	385	386
TEST OBJECTIVE	ENDURANCE TESTING	SHEET MOLD ELECTRODES	ENDURANCE TESTING	BULK KYNOL MATRIX
NO. CELLS	3	3	3	3
ANODE mg Pt/cm^2	.30 .28 .30	.24 .26 .21	.28 .27 .29	.27 .29 .28
CATHODE mg Pt/cm^2	.55 .61 .62	.53 .55 .54	.69 .63 .62	.51 .48 .51
MATRIX	SiC	KYNOL	SiC	BULK KYNOL (MASS PROD.)
PLATES/CONDITION	GOOD	GOOD	GOOD	GOOD
PEAK PERFORMANCE (Volts) Air-	.54 .54 .54	.62 .61 .62	.61 .60 .59	.47 .55 .54
PEAK PERFORMANCE (Volts) OCV-	.86 .78 .80	.88 .89 .88	.75 .76 .77	.75 .89 .90
PRESENT PERFORMANCE (Volts) Air-		.59 .60 .58	.59 .53 .54	.49 .55 .51
PRESENT PERFORMANCE (Volts) OCV-		.80 .84 .84	.74 .77 .70	.79 .86 .87
O_2 GAIN (Volts)	.11 .09 .08	.07 .07 .07	.09 .08 .09	.18 .11 .16
INITIAL mΩ READING	6.8	6.2	6.2	6.9
ACID HISTORY, hrs		ACID SUPPLY REMOVED	INITIAL WICK IN PROGRESS	END INITIAL WICK, 100
GAS UTILIZATION/ SENSITIVITY			H_2 SENSITIVE	H_2 SENSITIVE
TOTAL HOURS	68	915	314	148
REMARKS	DISASSEMBLED	STACK TORQUED AT 651 HRS AT 100 mA/cm^2	AT 100 mA/cm^2	AT 100 mA/cm^2

TABLE III.4 STACK TESTING SUMMARY

- Active Testing Update
- 108 ASF (40 A)

STACK NO.	387					
TEST OBJECTIVE	MULTIPLE CURRENT CONTACTS					
NO. CELLS	3					
ANODE mg Pt/cm^2	.30	.28	.28			
CATHODE mg Pt/cm^2	.61	.57	.63			
MATRIX	SiC					
PLATES/CONDITION	GOOD					
PEAK PERFORMANCE (Volts) Air-	.60	.61	.62			
PEAK PERFORMANCE (Volts) OCV-	.80	.84	.85			
PRESENT PERFORMANCE (Volts) Air-	.57	.54	.64			
PRESENT PERFORMANCE (Volts) OCV-	.75	.70	.84			
O_2 GAIN (Volts)	.08	.08	.05			
INITIAL mΩ READING	5.0					
AIR HISTORY, hrs	INITIAL WICK IN PROGRESS					
GAS UTILIZATION/ SENSITIVITY						
TOTAL HOURS	148					
REMARKS						

was monitored when the stack was steady at 177°C each time. It was observed that the resistance of the stack decreased from 5.1 mΩ at 15 psi to 4.7 mΩ at 35 psi while the total performance gain was 20 mV. Initial performance of the stack at 35 psi was 607 mV at 112 mA/cm^2.

The stack was finally torqued down to 40 psi with no change in performance, then disassembled after 29 hours of operation. The backing paper was not observed to be leaking any acid.

Similar experiments were conducted on Stack 381. Figure III.2 shows the ohmic resistance of the stack as a function of temperature and Figure III.3 represents the stack as a function of compression at OCV and 112 mA/cm^2. As the temperature and compression increase, the ohmic resistance decreases. Stack ohmic resistance was reduced from 5.8 mΩ to 4.8 mΩ by changing the compression from 15 psi to 35 psi.

At 40A current, the performance gain is calculated to be 40 mV due to the reduction of ohmic resistance. The terminal voltage gain was observed to be 40 mV (1.86 V to 1.90 V) which can be attributed to the reduction of ohmic resistance.

These experiments lead to the following conclusions:

- The internal resistance of a stack depends on the components, shim thickness and compression applied on the stack.
- If the stack is torqued in a controlled manner, the ohmic resistance can be reduced to a reasonably low value, acid leakage through the backing paper can be avoided, and the performance can be improved. An optimum compression of 55 psi $\pm$ 5 psi was selected for the compression of the subsequent stacks.

3.3.2 Effect of Reformed Fuel

Stack 369 has been studied with simulated reformed fuel (SRF). The simulated reformed fuel (SRF) composition was maintained at 72.5% H_2, 23.6% CO_2, 3.4% H_2O and 0.5% CO. Average cell performance of the stack was 580 mV. The immediate loss

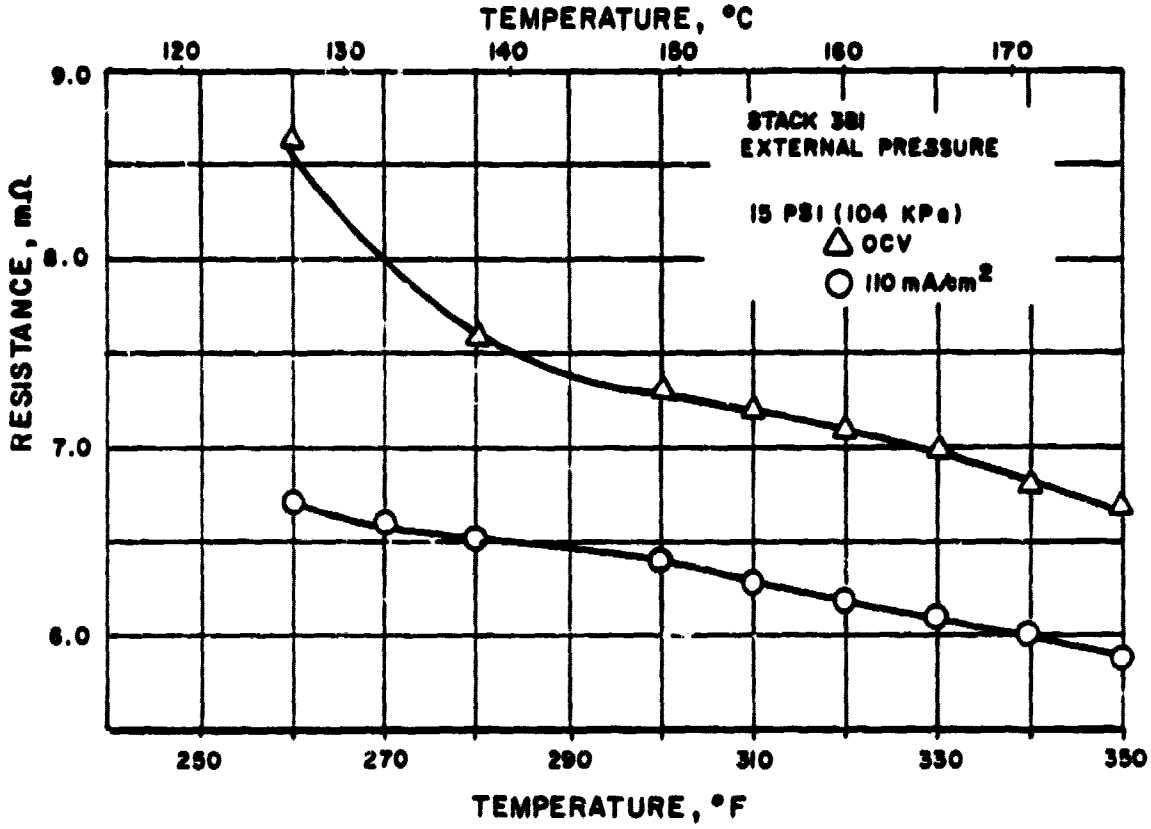

FIGURE III.2 OHMIC RESISTANCE AS A FUNCTION OF TEMPERATURE

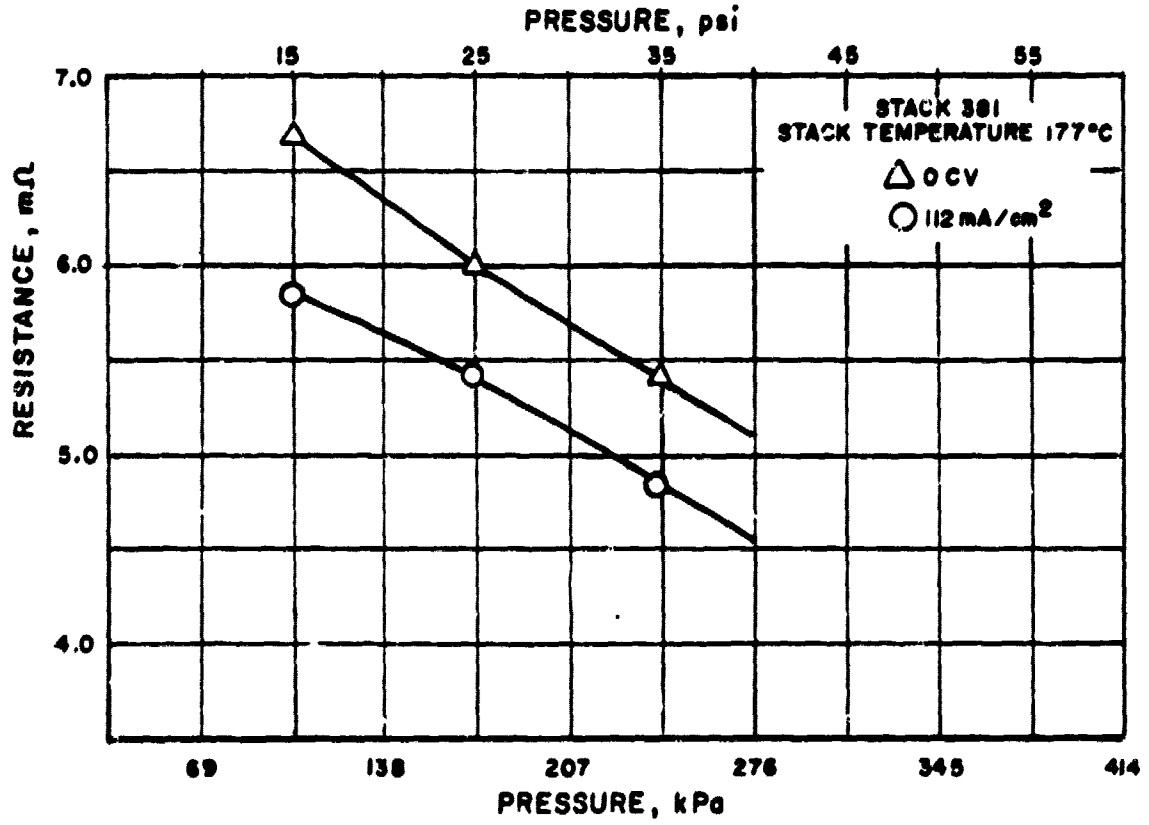

FIGURE III.3 OHMIC RESISTANCE AS A FUNCTION OF COMPRESSION

of performance observed was about 20 mV because of a change in fuel gas from 1.25 stoich of pure hydrogen to 1.25 stoich of SRF. An arithmetic average of the inlet and outlet Nernst loss for this SRF composition is 13.5 mV. The remaining 6.5 mV could be attributed to the presence of CO. After 800 hours, changing the SRF to pure H_2 regained the original performance. This is in agreement with previous testing of CO effects.

3.3.3 Effect of Current Density

During periods of high power demand a stack is required to operate at higher load. At high load the stack operates at higher current density and lower potential. At low cathode potentials, undesirable carbon corrosion and platinum dissolution decrease which results in a low rate of performance decay. Depending on potential and power requirements, an optimum current density operation at higher loads is desirable. In this connection and in view of our design point, Stack 349 was operated at 150 mA/cm^2 to study endurance, performance and stability. Current density of the stack was increased from 100 mA/cm^2 (performance of 597 mV/cell) to 150 mA/cm^2 with a performance of 560 mV/cell. Stack performance reached 570 mV/cell at 150 mA/cm^2 after 2700 hours of operation. Later, one of the cells developed low OCV which resulted in termination of the test after 3300 hours. Performance of the stack was 560 mV. No loss of performance was observed due to the high current operation and the stack performance was quite stable.

3.3.4 Preheated Hydrogen

Experiments have been designed to determine if there is any performance gain by preheating the fuel gas. Temperature profiles in Stack 380 have been obtained for hydrogen entering at room temperature (20°C) and at a preheated 110°C. During

these experiments, no observable performance gain was noticed between hot and cold hydrogen for 12.7 cm x 38.1 cm stacks.

Figure III.4 shows the temperature profiles for Cell No. 2 of Stack 381 for cold and hot hydrogen. No performance gain between the cold (20°C) and hot (110°C) hydrogen was observed. Examination of the temperature profiles in the cells indicates that not much difference between the two conditions was created except at the fuel entrance. The reason for this may be the smaller mass flow rates of the fuel. However some change in performance is expected in large area stacks with preheated hydrogen.

3.4 Component Evaluation

Component evaluation in stack testing during this quarter can be divided as follows:

Effect of Teflon in Electrodes

Sheet Mold Electrodes

Wet Assembly of SiC Stacks

3.4.1 Effect of Teflon in Electrodes

Experiments have been conducted to determine the effect of Teflon in the electrode layer. The performance of Stack 366 (50% Teflon in cathode) was compared with Stack 367 (45% Teflon in cathode). Lifegraphs of the stacks are shown in Figure III.5. Stack 366 started with a low initial performance (~0.55V), picked up considerably (~30 mV), and maintained that performance level (about 0.576V at 40A); whereas Stack 367 started with a higher initial performance (~0.575V), picked up slightly (~17 mV) and then started decaying gradually. It was operating at about 0.565V at a 40A level shortly before it was found overheated at 274°C. It was later terminated because of rapidly deteriorating performance. Additional testing is required.

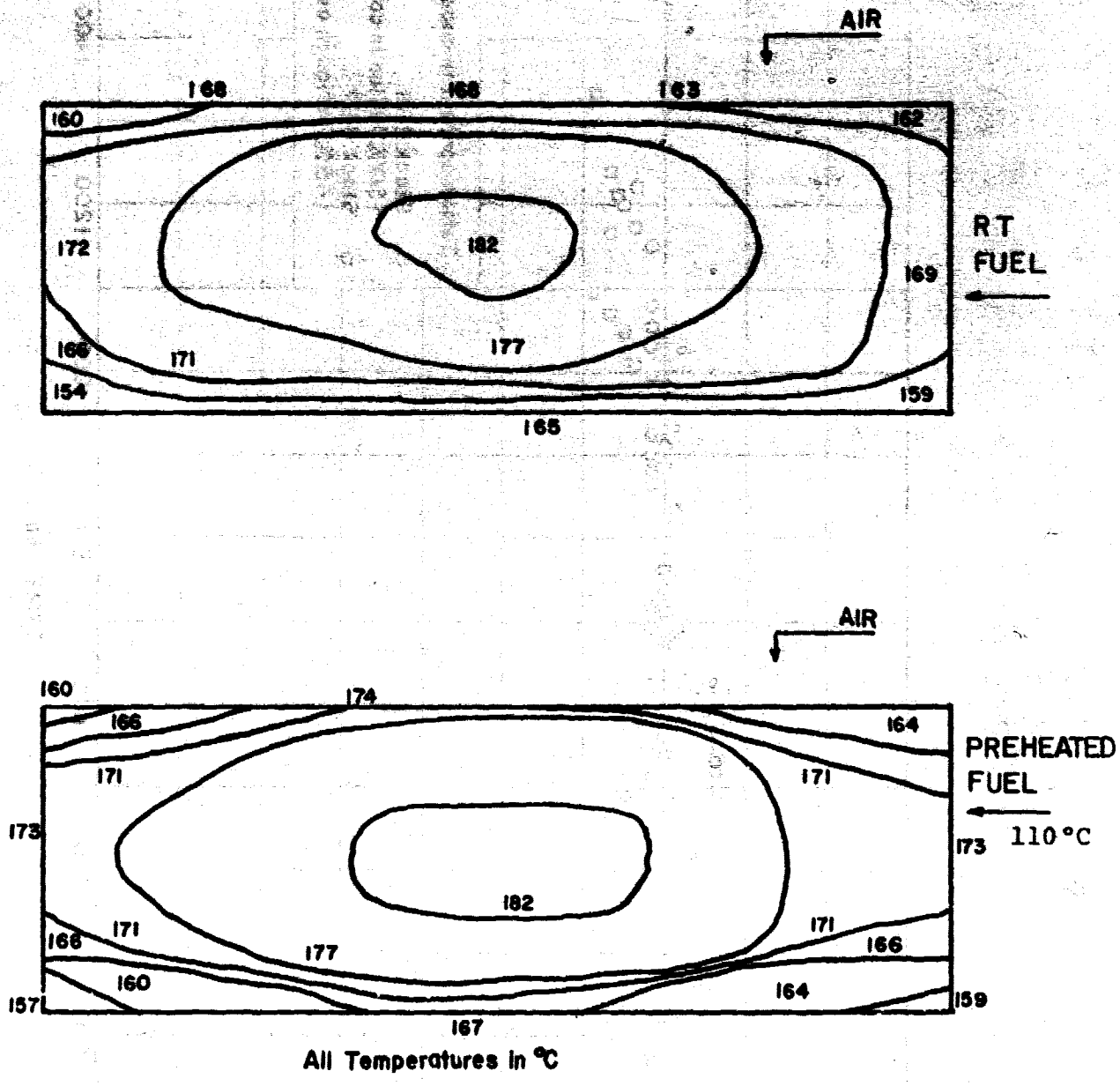

FIGURE III.4 TEMPERATURE DISTRIBUTION FOR ROOM TEMPERATURE AND PREHEATED H_2 (Stack 381, Cell #2)

D0620

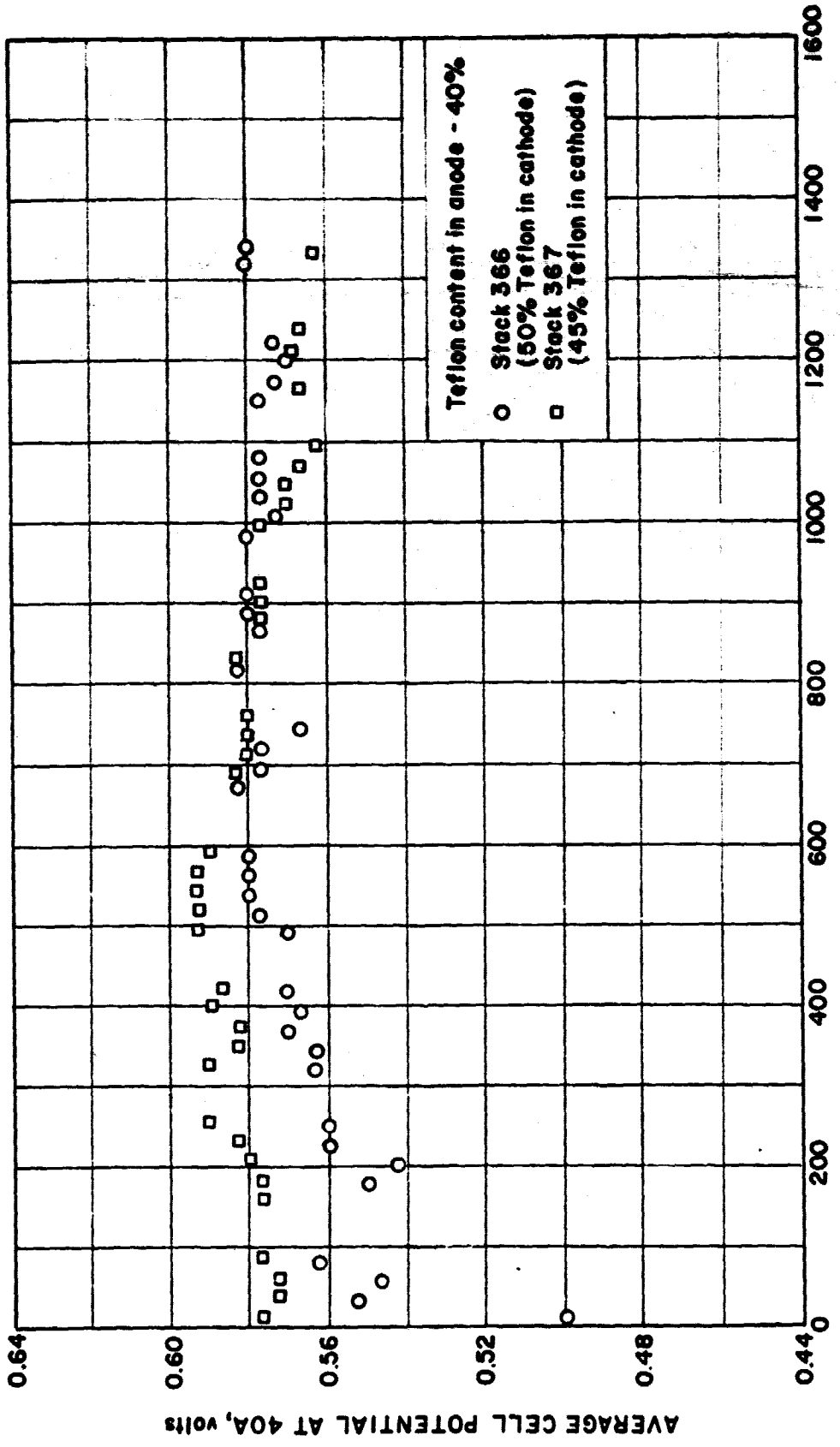

FIGURE III.5 LIFEGRAPHS OF STACKS 366 AND 367

3.4.2 Sheet Mold Electrodes

Two stacks (379 and 384) have been assembled with sheet mold electrodes. Stack 379, wet assembled with prefilled electrodes, achieved an initial performance of 0.64V at 112 mA/cm^2, an OCV reading of 0.89V, an ohmic resistance of 4.8 mΩ, and an O_2 gain of 60 mV at 112 mA/cm^2. The lifegraph for Stack 379 is shown in Figure III.6. After acid was added to the stack (because the prefilled electrodes appeared dry during assembly), performance dropped about 45 mV at 112 mA/cm^2 and the O_2 gain increased to 80 mV. The addition of acid may have caused flooding when the acid supply was removed. After 800 hours, the OCV started dropping and then developed cross-leaks while the performance began decreasing further. After 1300 hours of operation, the acid supply was put on and the stack appeared to be gaining in performance and OCV. At 1850 hours of operation, the polarization curve indicated 90 mV of O_2 gain. The acid supply was removed and the stack appears to be stable and slightly improved.

Stack 384 was also assembled with prewet components. The stack started with an initial performance of 0.61V but with a higher resistance (6.5 mΩ). Soon the performance began dropping and acid was added. The performance remained low until the stack was torqued, and the performance at 100 mA/cm^2 is now 0.59 mV.

Additional stacks will be tested with sheet mold electrodes for life and performance to compare the advantages and disadvantages of sheet mold over rolled electrodes.

3.4.3 Wet Assembly of SiC Matrix Stacks

Stacks with SiC matrices have been assembled with prefilled components. Stacks 377, 381, 383, 385 and 387 were wet-assembled.

Table III.5 describes the SiC stacks that are wet-assembled.

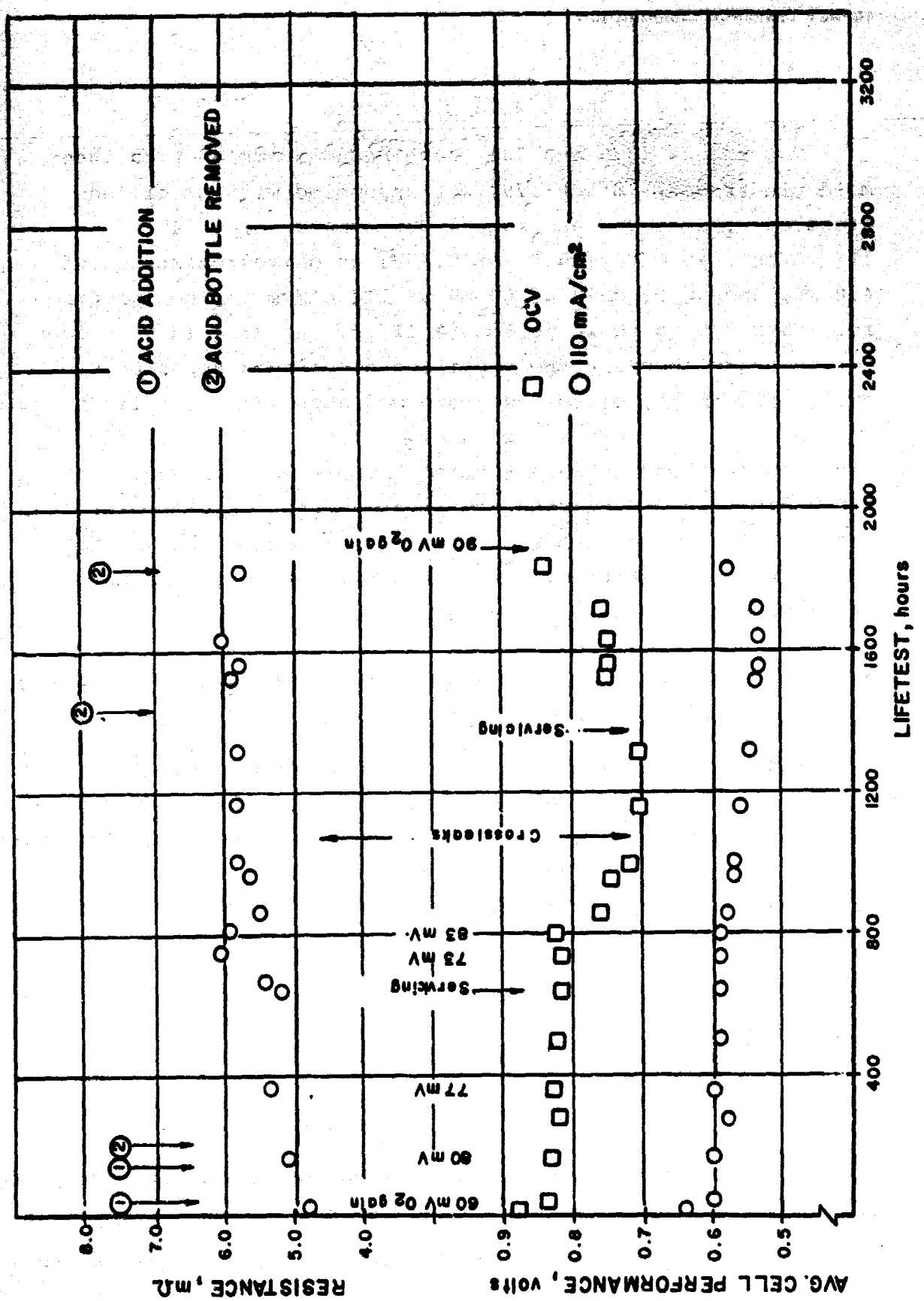

D0906

FIGURE III.6 LIFEGRAPH FOR STACK 379

ENERGY RESEARCH CORPORATION

TABLE III.5 PERFORMANCE OF WET-ASSEMBLED SiC STACKS

Stack	Purpose	Remarks
377	SiC prewet electrodes for 1 day, A-B plates.	Initial stack performance was 0.615 V at 112 mA/cm^2. However the stack required additional acid. Post-test analysis indicated that the acid replenishment was not achieved, due to a faulty end plate.
381	Prefilled component assembly, ohmic resistance measurement.	Initial stack performance was 0.62V at 112 mA/cm^2. Later performance decreased and ohmic resistance increased. Further torquing planned to decrease ohmic resistance.
383	Prefilled components, SiC matrix, AB plates, compression.	The stack, torqued consistently to approx. 60 psi, developed crossleaks at the final pressure. Post-test analysis indicated heavy compression on cathodes and acid leakage.
385	Prefilled components for longer time, A-B plates.	Started with low OCVs and cross-leaks. Electrodes may be flooded; crossleaks could not be repaired.
387	Prefilled components, multiple current collector tabs.	Presently steady at 0.59V.

TASK IV. SHORT STACK TESTING

Two 1200 cm^2 size short stacks have been assembled this quarter for testing. The summary is presented in Table IV.1.

- Performance Stability of Stack 406

The lifegraph for Stack 406 is shown in Figure IV.1. Initially the stack was started with known pressure between the tie rods. In about 250 hours of operation, the ohmic resistance of the stack went from 5.2 mΩ to 7.6 mΩ at the operating conditions, while average cell performance went from 0.54V to 0.46V (an 80 mV drop). The performance drop due to increase in resistance accounts for about 58 mV only; the drop in OCV may be the reason for the remaining 22 mV drop. Acid was supplied to the cells continuously because it was observed that the OCV of some cells started decreasing and crossleaking. After 300 hours of operation, the acid addition was stopped because it was no longer helping improve the cells. The cell was torqued which resulted in a performance gain, but further systematic torqueing did not noticeably improve the performance. (See Figure IV.1.)

Stack performance and stability will be followed in the subsequent reports.

TABLE IV.1 SUMMARY OF STACKS 406 AND 407

STACK NO.	PURPOSE AND ASSEMBLY	REMARKS
406	Stack was assembled with electrodes prefilled with a calculated amount of 98% acid. Thick copper was used as a current collector.	Stack has been running at about 0.52V terminal voltage for the last 800 hrs. The performance was as low as 0.47V per cell before it was torqued to 35 psi. (See Figure IV.1.)
407	Stack was assembled with dry electrodes and dry matrix. A provision was made for acid wicking.	Initial performance was good. Stack showed need for acid at 100 hrs. Average cell performance (over 130 hrs) is about 0.55V and is presently stable. Good acid wicking procedure. Acid channel exposure to gas may be causing the frequent drop in OCV.

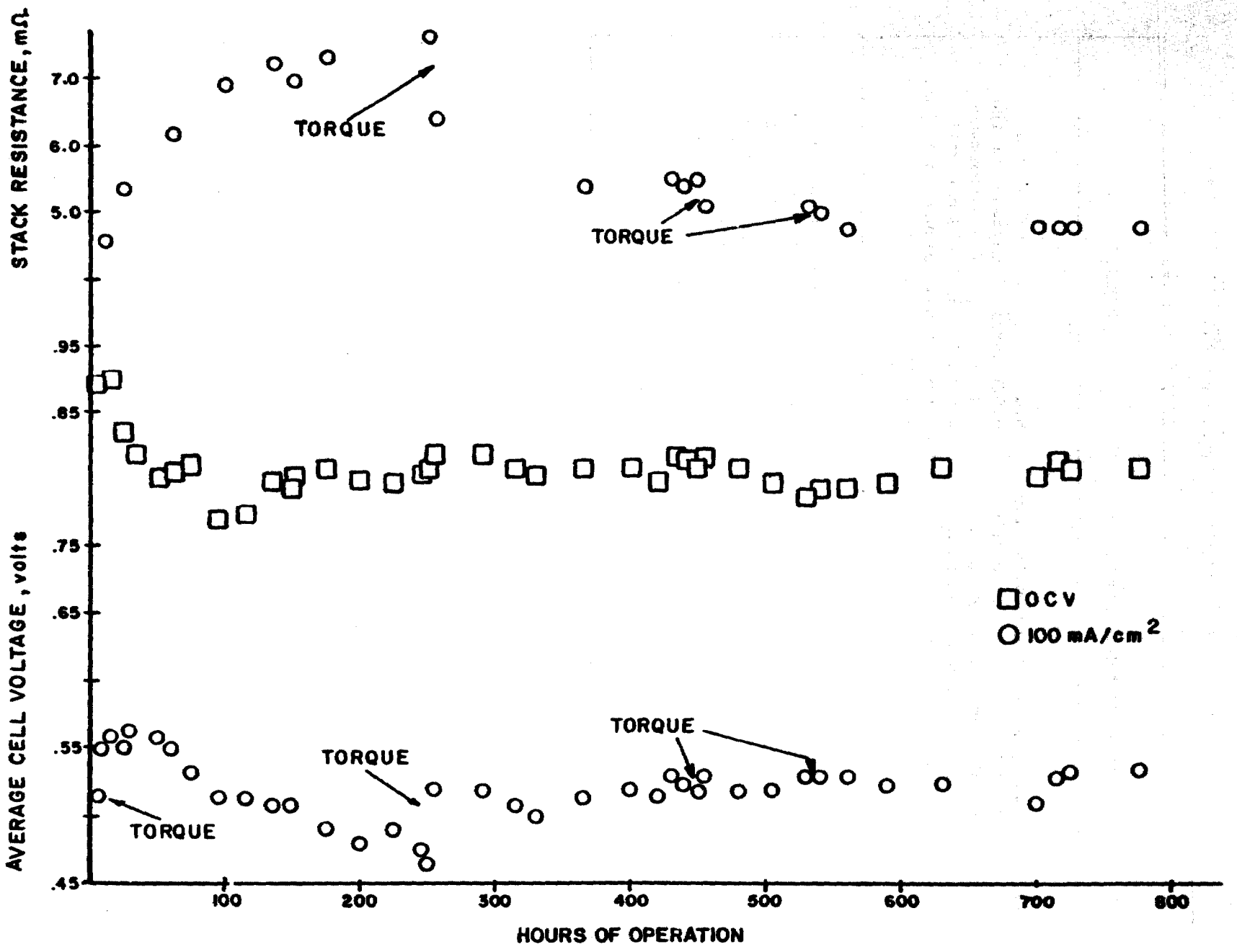

FIGURE IV.1 LIFEGRAPH FOR STACK 406

D0907

APPENDIX A Estimation of Cell Component Resistances

In an effort to evaluate IR contribution of each cell component to cell performance, component resistances in a 12.7 cm x 38.1 cm (5 in. x 15 in.) stack were estimated. The total resistance, R_T, can be expressed in terms of each component as follows (see Figure A1):

$$R_T = R^{at}_{cbt} + R_b + R^{at}_{cbp} + n\,R_p + (n-1)\left(R^{ac}_{cbpc} + R^{a}_{be} + R^{a}_{cea} + R_{acid} + R^{c}_{cea} + R^{c}_{be} + R^{ac}_{cbpa}\right) + R^{ct}_{cbp} + R_b + R^{ct}_{cbt}$$

where,

n = no. of bipolar plates

R^{at}_{cbt}, R^{ct}_{cbt} = contact resistances between backing paper and current collector terminal at anode side and cathode side

R_b = resistance of backing paper

R^{at}_{cbp}, R^{ct}_{cbp} = contact resistances between backing and anode ribs or cathode ribs at current collector terminals

R_p = resistance of bipolar plate

R^{ac}_{cbpa}, R^{ac}_{cbpc} = contact resistances between backing and cathode or anode ribs compressed between anode and cathode

R^{a}_{be}, R^{c}_{be} = resistances of composite backing and anode or cathode

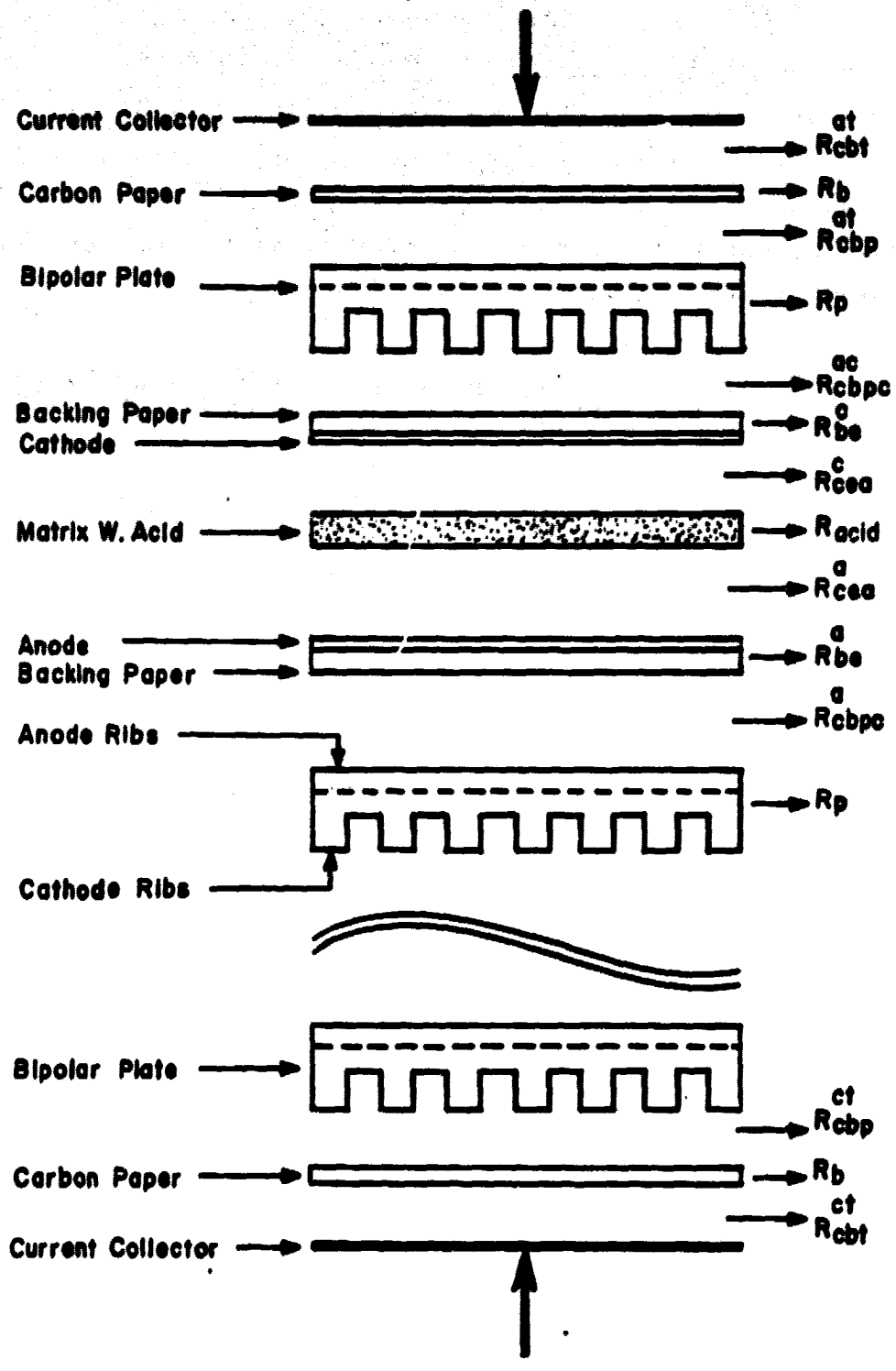

FIGURE A-1 EXPLODED VIEW OF COMPONENT RESISTANCES IN A FUEL CELL STACK

R^a_{cea}, R^c_{cea} = contact resistances between anode or cathode and acid in matrix

R_{acid} = resistance of acid in electrode and matrix

To separate contact resistance from total resistance measurements, the following equations were derived for resistances of bipolar plates and backing papers compressed between plates. (See Figure A2.)

L_1 and L_2 in the trapezoids can be expressed in terms of variable height x.

$$L_1 = \frac{a_1 - a_2}{h} x + a_2$$

$$L_2 = \frac{b_1 - b_2}{h} x + b_2$$

since,

$$R = \int_o^h P_R \frac{dx}{S(x)}$$

$$\therefore Rw \text{ (for web)} = \int_o^h P_R \frac{dx}{L_1 \bullet L_2} = \frac{h P_R}{(a_2 b_1 - a_1 b_1)} \ln \frac{a_2 b_1}{a_1 b_2}$$

For cathode rib,

$$R_c = \frac{P_R h_c}{a_2 (b_2 - b_0)} \ln \frac{b_2}{b_0}$$

For anode rib,

$$R_a = \frac{P_R h_a}{b_1 (a_1 - a_0)} \ln \frac{a_1}{a_0}$$

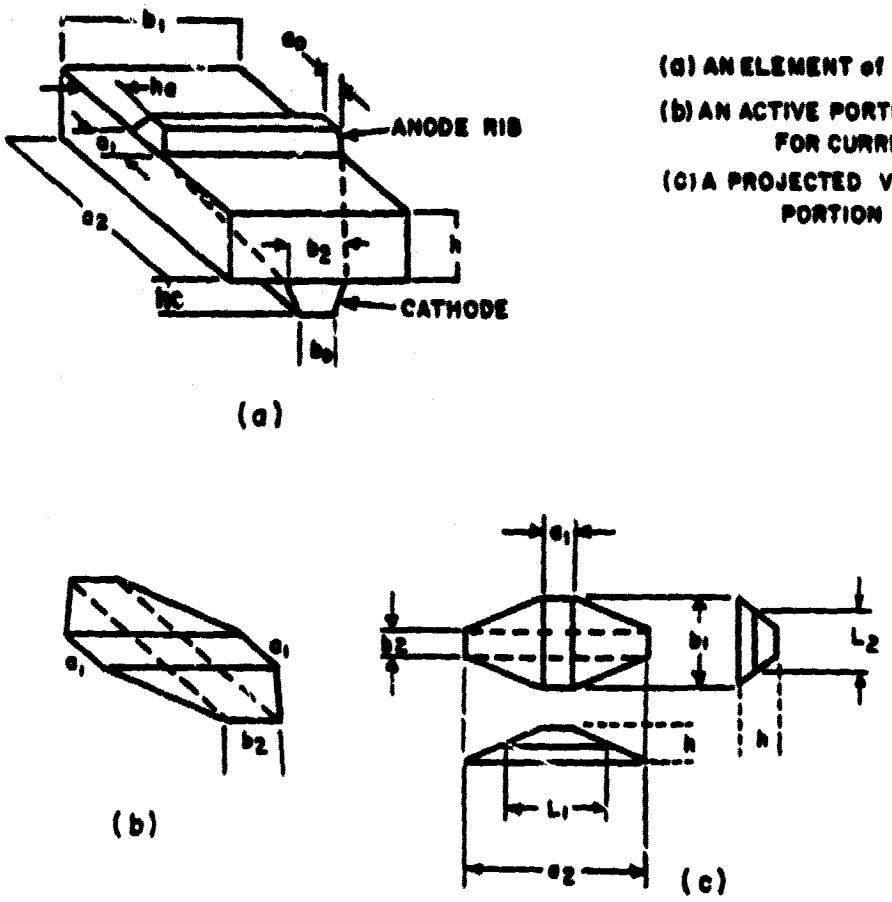

FIGURE A-2 SCHEMATIC VIEW OF A BIPOLAR PLATE ELEMENT

Where P_R (specific resistivity) was assumed to be uniform in all directions.

$$\therefore \text{Resistance of a bipolar plate} = \frac{(R_w + R_a + R_c)}{(\text{No. of } b_1 \times a_2 \text{ sized elements})}$$

For a backing paper compressed between anode and cathode ribs, an equation similar to R_w can be obtained.

$$R_b = \frac{h^1 P_R^1}{(a_2 b_1 - a_1 b_1)} \ln \frac{a_2 b_1}{a_1 b_2}$$

$$\therefore \text{Resistance of a backing paper} = \frac{R_b}{(\text{No. of } b_1 \times a_2 \text{ sized elements})}$$